Semi-global analysis of periodic and quasi-periodic normal-internal $k:1$ and $k:2$ resonances

K Saleh[1] **and FOO Wagener**[2]

[1] Dept of Mathematics, University of Groningen, PO Box 800, 9700 AV Groningen, The Netherlands, t: +31 50 363 3954

[2] CeNDEF, Dept of Quantitative Economics, University of Amsterdam, Roetersstraat 11, 1018 WB Amsterdam, The Netherlands, t: +31 20 525 4034, f: +31 20 525 4349

E-mail: khairul@math.rug.nl, wagener@uva.nl

Abstract. The present paper investigates a family of nonlinear oscillators at Hopf bifurcation, driven by a small quasi–periodic forcing. In particular we are interested in the situation that at bifurcation and for vanishing forcing strength, the driving frequency and the normal frequency are in $k:1$ or $k:2$ resonance. For small but nonvanishing forcing strength, a semi–global normal form system is found by averaging and applying a van der Pol transformation. The bifurcation diagram is organised by a codimension 3 singularity of nilpotent-elliptic type. A fairly complete analysis of local bifurcations is given; moreover, all the nonlocal bifurcation curves predicted by Dumortier [25] are found numerically.

AMS classification scheme numbers: 34C15, 34C20, 70K30, 70K43

Submitted to: *Nonlinearity*

1. Introduction

In appendix II of his book on nonlinear vibrations [46], Stoker considered a nonlinear oscillator with damping and quasi-periodic driving, of the form

$$\ddot{y} + c\dot{y} + y - \beta y^2 = f(\omega_1 t, \omega_2 t), \tag{1}$$

with f a 2π-periodic function in both arguments. If for given f the damping strength c is sufficiently large, or if for given c the function f is sufficiently small in some function norm, he showed, using a contraction argument, that this system has a so-called *response solution* $y(t) = \varphi(\omega_1 t, \omega_2 t)$, where φ is 2π-periodic in both arguments.

Stoker remarked that "the usual methods of approximation applied to equation (1) for $c = 0$ (i.e. without damping) and ω_1/ω_2 irrational would almost certainly lead to divergent series because of the occurrence of certain small divisors in the representation of the terms in the series expansions". This question, of whether response solutions exist in equations like (1) for c close to 0, is nowadays called 'Stoker's problem'.

1.1. Stoker's problem at strong resonances

After Moser [43, 26] solved Stoker's problem for reversible systems, Braaksma and Broer [3] considered Stoker's problem for families of general nonlinear oscillators; in that context, Stoker's problem asks for the persistence of the 'central' invariant torus near Hopf bifurcation parameter values. They showed the existence of a Hopf bifurcation set $\mathcal{H}_c$ which is a positive measure subset of a codimension 1 submanifold $\mathcal{H}$ in parameter space. Also, by applying centre manifold theory, they showed that there are two open parameter sets $\mathcal{A}$ and $\mathcal{R}$, one at either side of $\mathcal{H}$, having infinite order of contact at $\mathcal{H}_c$. The system has an normally hyperbolic invariant m-dimensional torus, attracting for parameter values in $\mathcal{A}$, repelling for values in $\mathcal{R}$. Moreover, depending on whether the Hopf bifurcation is subcritical or supercritical, there are similar smaller open subset $\mathcal{R}^+ \subset \mathcal{R}$ (subcritical case) or $\mathcal{A}^+ \subset \mathcal{A}$ (supercritical case), also having infinite order of contact with $\mathcal{H}$ at $\mathcal{H}_c$, such that for parameters in these sets, the system has a normally hyperbolic repelling (for parameter values in $\mathcal{R}^+$) or attracting (values in $\mathcal{A}^+$) torus of dimension $m+1$. All these invariant tori are finitely differentiable; the size of the sets $\mathcal{A}$, $\mathcal{A}^+$, $\mathcal{R}$ and $\mathcal{R}^+$ decreases as the degree of differentiability of the tori increases. See for more details [3, 10, 11].

We are interested in the complement of these sets, that is, we are interested in the set of parameters for which standard KAM theory and centre manifold theory do not yield the existence of invariant tori. In the case of a two parameter family, this complement consists of countably many so-called resonance holes (or bubbles), that are similar to the 'resonance bubbles' found in the case of the quasi-periodic saddle-node bifurcation by Chenciner [19, 20, 21]. We extend work by Gambaudo [27] and Wagener [53] on strong $k:\ell$ resonances with $k \in \mathbb{Z}^m$ and $\ell = 1, 2$. These articles study semi-global bifurcations for periodically ($m=1$) and quasi-periodically ($m \geq 2$) perturbed driven damped oscillators near Hopf bifurcation for both $\ell = 1$ and $\ell = 2$; after appropriate averaging and truncation of the system, a $\mathbb{T}^m$-symmetry is divided out. A bifurcation analysis is performed of the remaining principal part at the (relative) equilibria for small pertubation strengths.

In the present article the bifurcation diagrams in the cases $\ell = 1$ and $\ell = 2$ are completed. For the first case, the bifurcation diagram is understood completely by taking the codimension 3 singularity of nilpotent-elliptic type [25], found in [53], as an organising centre. Consequently, we find a codimension 2 degenerate Hopf bifurcation, absent from [27, 53], whose existence is implied by the codimension 3 bifurcation (this was kindly pointed out to us by Freddy Dumortier). For both cases, we add curves of homoclinic and heteroclinic global bifurcations to the bifurcation diagrams, that have been determined numerically by AUTO [22] and Matlab [31]. For $\ell \geq 3$ techniques from 'standard' KAM theory (cf. [3, 7, 11, 34, 35]) can be applied to show the existence of invariant tori.

The first step of the analysis of the quasi-periodic case is the analysis of the periodic case. Though these two cases are strongly related the quasi-periodic case is

more involved than the periodic case, since the set of resonating normal frequencies is dense in the set of all normal frequencies. This implies that the overall picture has a lot more fine-structure; we shall be more precise below.

1.2. Relation to previous work

Response solutions of periodically driven damped non-harmonic oscillators at resonance have already been studied by van der Pol [51], Cartwright and Littlewood (e.g.[17, 18]) and in Stoker's monograph on nonlinear vibrations ([46, p. 107ff, p. 114ff and Figure 3.1 on p. 92]). See also [9, 16].

For a systematic bifurcation analysis of these resonances see [47], where, using normal form theory, the generic strong ($1:\ell$ for $\ell = 1, \cdots, 4$) and weak ($\ell \geq 5$) resonances of periodic response solutions at non-degenerate Hopf bifurcation are classified and described. For the $1:4$ resonances, see [1, 36, 37, 38, 39]. We refer the reader to the overview given in [1, §35, p. 302ff].

The $1:1$ resonance, also investigated in [4, 5], gives in this way rise to the Bogdanov-Takens bifurcation. However, from a practical point of view, the Bogdanov-Takens bifurcation does not describe fully what happens generically to the response solutions of a driven damped oscillator at resonance: for some parameter values, there are two response solutions, for others there are none. Under natural hypotheses, for instance if the friction coefficient grows sufficiently quickly with amplitude, a topological argument based on index theory [42] can be employed to show the existence of at least one response solution in the oscillator.

Besides the response solutions involved in the Bogdanov-Takens bifurcation there is yet another response solution, which for parameter values close to the Bogdanov-Takens bifurcation value is 'far away' from the bifurcating response solutions, and this third solution is therefore not captured by a local analysis. Holmes and Rand [33, 29] made a semi-global analysis of the $1:1$ resonance in a special case (our case $\vartheta = 0$) that captured all response solutions. We use the term 'semi-global' to indicate that after averaging and scaling, we consider phenomena in a given 'big' region of the phase space, rather than in the infinitesimally small regions sufficient for purely local bifurcation analysis.

The analysis of Holmes and Rand was extended by Gambaudo [27] to a semi-global bifurcation analysis of the generic codimension 2 cases of strong resonances at non-degenerate Hopf bifurcations. We note as an aside that recently a beginning has been made at analysing resonances of periodic response solutions at degenerate Hopf bifurcations [8]. In that case $1:\ell$ resonances are strong if $\ell \leq 6$ and weak otherwise. As we find families of degenerate Hopf bifurcations in our analysis, we expect that the phenomena reported in [8] will occur generically in our system as well.

In [53] the semi-global analysis of driven damped anharmonic oscillators at Hopf bifurcation has been taken up in the case that the driving is quasi-periodic instead of periodic. As mentioned before, in the first step of such an investigation 'averaging' or

'normal-form' techniques are applied [1, 48, 15, 16, 39] that permit to write the system as a periodically forced system with a small quasi-periodic perturbation term. Working in a different parametrisation from the one used in [33, 29, 27], and considering a third natural parameter, the analysis of the periodic part yielded that in the $1:1$ resonance, the two generic cases reported by Gambaudo can be seen as subfamilies of a generic three-dimensional bifurcation diagram that is organised by a singularity of nilpotent-elliptic type [25].

The present article completes the analysis started in [53], taking the nilpotent-elliptic point as 'organising centre' of the bifurcation diagram and exploring its implications, one of which is the occurrence of degenerate Hopf bifurcations in the $k:1$ resonance case. Also we compute all global bifurcation curves that are known from the analysis of the nilpotent-elliptic point, excepting those relating to 'boundary bifurcations'; these latter bifurcations concern tangencies of the vector field to the boundary of any small neighbourhood of the singularity [25].

Moreover, the consequences of the quasi-periodicity are spelled out more fully. For instance, in the periodic case the Hopf bifurcation set is a smooth manifold. In the quasi-periodic case, it is shown in [53] that every resonance between the perturbing quasi-periodic frequency and the Floquet exponent of the free oscillator generically gives rise to a resonance hole. Hence, in the quasi-periodic case it is to be expected that the Hopf bifurcation set is 'frayed'. We shall invoke quasi-periodic bifurcation theory [19, 11, 52] to investigate which portions of the local bifurcation diagram persist under small perturbations. In the bifurcation diagram there are quasi-periodic Hopf bifurcation sets for which the analysis of the article can be applied repeatedly: in this way resonance within resonances are found, as in, e.g., [2].

There are strong analogies between the present case of general (dissipative) nonlinear oscillators and the non-damped Hamiltonian case; in the history of the subject of nonlinear oscillations, the Hamiltonian case of a certain problem has usually been investigated before the dissipative case. Since equilibria with purely imaginary eigenvalues occur generically in Hamiltonian systems, strong $k:\ell$ resonances are already encountered in one-parameter families, and the bifurcation diagrams are consequently simpler. For a detailed analysis, we refer the reader to [9].

The present article is based on chapter 3 of [44]. An overview of the results obtained has been given in [13].

1.3. Overview

From the outset, attention is restricted to quasi-periodically damped driven systems. Examples are the system given in equation (1) and the forced Duffing–van der Pol oscillator

$$\ddot{y} + \left(a + cy^2\right)\dot{y} + by + dy^3 = \varepsilon f(\omega_1 t, \cdots, \omega_m t, y, \dot{y}, \sigma, \varepsilon),$$

where f is 2π-periodic in its first m arguments. This non-autonomous second order differential equation can be written as follows as a quasi-periodic perturbation of a

planar vector field:

$$\left\{\begin{array}{rcl} \dot{x}_j &=& \omega_j, \qquad j=1,\cdots,m, \\ \dot{y}_1 &=& y_2, \\ \dot{y}_2 &=& -\left(a+cy_1^2\right)y_2 - by_1 - dy_1^3 + \varepsilon f(x_1,\cdots,x_m,y_1,y_2,\sigma,\varepsilon). \end{array}\right. \tag{2}$$

Here $x \in \mathbb{T}^m = \mathbb{R}^m/2\pi\mathbb{Z}^m$ is usually called the *internal* variable, and $y_1 = y$ and $y_2 = \dot{y}$ are called *normal* variables; note that for system (2) the internal dynamics are independent of the normal variables. This allows us to focus attention on the interaction of normal and internal dynamics, without having to take care of internal resonances.

Vector fields. Generalising this example, we consider parametrised families of vector fields $X(\sigma,\varepsilon)$, with integral curves in the phase space $\mathbb{T}^m \times \mathbb{R}^2$, of the form

$$X(\sigma,\varepsilon) = \omega\frac{\partial}{\partial x} + Z = \omega\frac{\partial}{\partial x} + \Big(A(\sigma)y + B(y,\sigma) + \varepsilon F(x,y,\sigma,\varepsilon)\Big)\,\frac{\partial}{\partial y}. \tag{3}$$

As in the example $x \in \mathbb{T}^m$ is called the internal (or torus) coordinate, and $y \in \mathbb{R}^2$ the normal coordinate. The vector $\omega \in \mathbb{R}^m$ (assumed constant) is called the (internal) frequency vector, which will be assumed to be quasi-periodic; the notation $\omega\frac{\partial}{\partial x}$ is shorthand for $\sum_{i=1}^m \omega_i \frac{\partial}{\partial x_i}$. Moreover, $\sigma \in P \subset \mathbb{R}^q$ is a multi-dimensional (system) parameter, ranging over an open and bounded subset P of $\mathbb{R}^q$, and $\varepsilon \in (-\varepsilon_0,\varepsilon_0)$ is traditionally known as the perturbation strength. Note that by assumption, the natural projection of the system flow to $\mathbb{T}^m$ is always quasi-periodic. All functions are assumed to depend infinitely differentiably (or smoothly) on their arguments. Finally, with $|y|$ denoting the Euclidean norm of y, the term B is assumed to be of order $\mathsf{O}(|y|^2)$ in y, uniformly in σ.

For instance, the forced Duffing–van der Pol oscillator (2) fits in this framework if we set $\sigma = (a,b,c,d)$ and

$$A(\sigma) = \begin{pmatrix} 0 & 1 \\ -b & -a \end{pmatrix}, \quad B(y,\sigma) = \begin{pmatrix} 0 \\ -cy_1^2y_2 - dy_1^3 \end{pmatrix},$$
$$F(x,y,\sigma,\varepsilon) = \begin{pmatrix} 0 \\ f(x,y,\sigma,\varepsilon) \end{pmatrix}.$$

Integrable systems. Consider the action τ of the group $\mathbb{T}^m$ on $\mathcal{M}$ that is given by

$$\tau_\xi(x,y) = (x+\xi, y),$$

for $\xi \in \mathbb{T}^m$, cf. [11]. A vector field Y is called symmetric (or equivariant) with respect to τ, that is, invariant under the induced action of τ, if $(\tau_\xi)_* Y = Y$ for all $\xi \in \mathbb{T}^m$. In analogy to the situation for Hamiltonian systems, a symmetric vector field is said to be *integrable*.

Note that for $\varepsilon = 0$, the family $X_0 = X_0(\sigma) = X(\sigma,0)$ is symmetric. Moreover, the vector field X_0 is tangent to the torus $\mathcal{T} = \mathbb{T}^m \times \{0\}$; this implies that the torus $\mathcal{T}$ is invariant under the flow of X_0. The normal linear stability of the invariant torus $\mathcal{T}$ is

controlled by the linear part $A(\sigma)y\frac{\partial}{\partial y}$ of the normal part Z_0 of X_0 at $y=0$. Note that the integrable vector field $X_0(\sigma)$ is always in (quasi-periodic) Floquet form: the normal linear part $\omega\frac{\partial}{\partial x}+A(\sigma)y\frac{\partial}{\partial y}$ of $X_0(\sigma)$ at $\mathcal{T}$ is independent of $x\in\mathbb{T}^m$.

Dividing out the torus symmetry reduces X_0 to a planar vector field, which is identified with the normal part $Z_0(\sigma)=Z(\sigma,0)$ of the integrable vector field X_0. Studying $X(\sigma,\varepsilon)$ for $\varepsilon\neq 0$ amounts to investigating a non-integrable perturbation of the integrable family of vector fields $X_0(\sigma)$.

Resonances in Hopf bifurcations. It is assumed that for some value σ_0 of the parameter σ the normal part Z_0 of X_0 versally unfolds a Hopf bifurcation singularity at $y=0$. Denote the eigenvalues of $A(\sigma)$ by $\mu(\sigma)\pm\mathrm{i}\alpha(\sigma)$.

A normal-internal $k:\ell$ resonance of the invariant torus $\mathcal{T}$ is a relation of the form

$$\langle k,\omega\rangle+\ell\alpha(\sigma_0)=0 \tag{4}$$

between ω and $\alpha(\sigma_0)$, where $k\in\mathbb{Z}^m$ and $\ell\in\mathbb{Z}$ are not both equal to 0; here $\langle\cdot,\cdot\rangle$ denotes the standard inner product. The smallest value of $|\ell|$, where ℓ ranges over all integers, for which there is a $k\in\mathbb{Z}^m$ such that (4) holds is called the order of the resonance. Resonances of order up to 4 are called strong resonances in the present context (cf. [47]); higher order resonances are called weak. If for $\sigma=\sigma_0$ the torus $\mathcal{T}$ is respectively non-resonant, weakly resonant or strongly resonant, the value σ_0 is called a non-degenerate, weakly resonant or strongly resonant quasi-periodic Hopf bifurcation value.

We have already mentioned that the non-degenerate as well as the weakly resonant quasi-periodic Hopf bifurcation have been investigated by Braaksma and Broer [3] for strongly non-resonant or *Diophantine* internal frequency vectors ω. For small positive values of the perturbation strength ε, they have found a codimension 1 submanifold $\mathcal{H}$ in the space of parameters, carrying a quasi-periodic Hopf bifurcation set $\mathcal{H}_c$ that has positive measure in $\mathcal{H}$, such that at every point σ of the bifurcation set, two open regions $\mathcal{A}_\sigma$ and $\mathcal{R}_\sigma$ in the complement of $\mathcal{H}$ and separated by $\mathcal{H}$ meet with infinite order of contact. For parameter values in $\mathcal{A}_\sigma$, the vector field has an attracting normally hyperbolic m-dimensional invariant torus close to $\mathcal{T}$, for values in $\mathcal{R}_\sigma$, a repelling one.

In the union of all sets $\mathcal{A}_\sigma$ and $\mathcal{R}_\sigma$, normal hyperbolic m-dimensional tori have thus been shown to exist. The complement of this union is usually referred to as the set of 'resonance holes' or 'Chenciner bubbles', in analogy to the *bulles* that Chenciner encountered in his analysis of the quasi-periodic saddle-node bifurcations [19, 20, 21]. It should be noted that these bubbles are proof-generated. In the case of the quasi-periodic saddle-node bifurcation, the relation between bubbles and internal resonances of invariant tori has been studied by Chenciner in [21]; the present article investigates for the quasi-periodic Hopf bifurcation the structure of the bifurcation diagram in these bubbles.

Normal forms. We are interested in the case that σ_0 is a strongly $k:1$ or $k:2$ resonant bifurcation value. For small values of ε, the form of the vector fields is first simplified by normal form (or averaging) transformations [6, 11, 45]. In section 3, the vector field is reduced to the special case that its normal frequencies are close to zero, by applying a *van der Pol transformation* [1, 9, 16, 51] and an appropriate scaling; the details of the transformation are relegated to Appendix B. After these transformations, the vector field takes the form

$$X = \delta^{-2}\omega\frac{\partial}{\partial x} + Z_0(\sigma) + \delta Z_1(\sigma,\delta) + \delta^N Z_2(\sigma,\delta).$$

Here $\delta = \varepsilon^{\frac{1}{4-\ell}}$ is another perturbation parameter; the vector fields $X_0 = \delta^{-2}\omega\frac{\partial}{\partial x} + Z_0$ and $\delta^{-2}\omega\frac{\partial}{\partial x} + Z_0 + \delta Z_1$ are integrable, and the power N can be chosen in advance; however, the transformations and their domain of definition will in general depend on N. By these transformations, quasi-periodicity has been pushed to terms of order δ^N. In fact, since X_0 is integrable, its *normal* or *principal part* dynamics Z_0 are decoupled from the torus dynamics. In complex coordinates $z = y_1 + \mathrm{i}y_2$, the vector field Z_0 reads modulo some scalings as

$$Z_0 = \mathrm{Re}\,\left(\lambda z + \mathrm{e}^{\mathrm{i}\vartheta}|z|^2 z + \bar{z}^{\ell-1}\right)\frac{\partial}{\partial z}\,.$$

The article proceeds as follows: in section 4, a complete local bifurcation analysis and a fairly comprehensive numerical global bifurcation analysis of the family Z_0 are given for the case $\ell = 1$, extending the work of [27, 53]. A codimension 3 singularity of nilpotent-elliptic type is found to be the organising centre of the bifurcation diagram. A brief description of this bifurcation, following [25], is given in Appendix A. The much shorter section 5 completes the local bifurcation diagram in the case $\ell = 2$, already given in [27, 53], by adding global bifurcation curves and giving the corresponding phase portraits.

Standard perturbation arguments imply that for small δ, the local bifurcation diagram for Z_0 is qualitatively the same as that for $Z_0 + \delta Z_1$; if the numerical evidence for the nondegeneracy of the global bifurcations is accepted, the same conclusion can be drawn for the global bifurcation manifolds. If furthermore the term $\delta^{-2}\omega\frac{\partial}{\partial x}$ is added, the bifurcation diagrams remain the same, but the interpretation changes: equilibria and limit cycles of the planar system $Z_0 + \delta Z_1$ correspond to respectively m-dimensional and $(m+1)$-dimensional quasi-periodic tori of

$$X_0 = \delta^{-2}\omega\frac{\partial}{\partial x} + Z_0 + \delta Z_1.$$

Adding the term $\delta^N Z_2$ breaks the $\mathbb{T}^m$-symmetry, and quasi-periodic bifurcation theory has to be invoked to investigate which portions of the local bifurcation diagram persist under this perturbation (section 6).

Now, in the quasi-periodic bifurcation diagram there are quasi-periodic Hopf bifurcation sets for which the analysis of the article can be applied again: in this way resonances within resonances are found. Section 6.3 investigates this iteration, which

can be performed at least finitely many times. Appendix B gives full details on the averaging and van der Pol transformations used in section 2.

2. Preliminary remarks

In this section notation is introduced, and some preliminary transformations are applied to the family of vector fields under consideration.

2.1. Assumptions

As above, we consider vector fields $X(\sigma,\varepsilon)$ on $\mathbb{T}^m \times \mathbb{R}^2$ which are of the form (3). Unless explicitly stated otherwise, in the following all functions are assumed to depend smoothly, that is infinitely differentiably, on their arguments. The following assumptions are made about $X(\sigma,\varepsilon)$.

Diophantine condition. The frequency vector $\omega \in \mathbb{R}^m$ is assumed to satisfy a *Diophantine condition of type* $D(\gamma,\tau)$: there are constants $\gamma > 0$, $\tau > m-1$, fixed for the remainder of the article, such that for all $k \in \mathbb{Z}^m \backslash \{0\}$:

$$|\langle k,\omega\rangle| \geq \gamma |k|^{-\tau}.$$

Normal linear dynamics. For the unperturbed system ($\varepsilon = 0$), the torus $\mathcal{T} = \{(x,y) \in \mathcal{M} : y = 0\}$ is invariant, and the normal linear dynamics of X at $\mathcal{T}$ are given by

$$N_{\mathcal{T}}(X) = \omega\frac{\partial}{\partial x} + A(\sigma)y\frac{\partial}{\partial y}.$$

The aim of the present article is to analyse non-degenerate Hopf bifurcations at normal resonances. At a Hopf bifurcation parameter value σ_0, the eigenvalues $\lambda_j(\sigma)$, $j = 1,2$ of $A(\sigma)$ are purely imaginary; by convention λ_1 denotes the eigenvalue with positive imaginary part. The map $\sigma \mapsto (\operatorname{Re}\lambda_1(\sigma), \operatorname{Im}\lambda_1(\sigma))$ is assumed to have surjective derivative at σ_0. Without loss of generality it can be assumed that $A(\sigma)$ is of the form

$$A(\sigma) = \begin{pmatrix} \mu & -\alpha \\ \alpha & \mu \end{pmatrix},$$

where $\sigma = (\mu,\alpha,\cdots)$, and that the parameter space P is such that α is positive and bounded away from 0. Under these assumptions the eigenvalues of $A(\sigma)$ are $\lambda_1 = \mu + \mathrm{i}\alpha$ and $\lambda_2 = \mu - \mathrm{i}\alpha$.

2.2. Preliminary transformations

As usual in this kind of problems, it is more convenient to replace real valued normal coordinates $y \in \mathbb{R}^2$ with complex valued coordinates $z \in \mathbb{C}$.

Complex notations. There will be a distinction between $f(z)$ and $f(z,\bar{z})$. The former will refer to an analytic function of its argument, while the latter will usually denote only a smooth function. Introduce the Wirtinger derivatives

$$\frac{\partial}{\partial z}=\frac{\partial}{\partial x}-\mathrm{i}\frac{\partial}{\partial y},\quad \text{and } \frac{\partial}{\partial \bar{z}}=\frac{\partial}{\partial x}+\mathrm{i}\frac{\partial}{\partial y};$$

then smoothness of $f(z,\bar{z})$ means that all derivatives

$$\frac{\partial^{\beta_1+\beta_2} f}{\partial z^{\beta_1}\partial \bar{z}^{\beta_2}}$$

exist and are continuous. By setting $z=y_1+\mathrm{i}y_2$ and

$$f(z,\bar{z})=f_1(\mathrm{Re}\, z,\mathrm{Im}\, z)+\mathrm{i}f_2(\mathrm{Re}\, z,\mathrm{Im}\, z),$$

the planar system of real differential equations

$$\dot{y}_1=f_1(y_1,y_2),\qquad \dot{y}_2=f_2(y_1,y_2),$$

is seen to be equivalent to the complex differential equation

$$\dot{z}=f(z,\bar{z}).$$

With the same notations, the corresponding vector field is seen to satisfy

$$f_1(y_1,y_2)\frac{\partial}{\partial y_1}+f_2(y_1,y_2)\frac{\partial}{\partial y_2}=\mathrm{Re}\, f(z,\bar{z})\frac{\partial}{\partial z}.$$

In this sense, we say that the vector field $\mathrm{Re}\, f\frac{\partial}{\partial z}$ corresponds to the differential equation $\dot{z}=f$.

Vertical vector fields. Using this notation, and setting $z=y_1+\mathrm{i}y_2$ and $\lambda=\mu+\mathrm{i}\alpha$, the vector field X takes the form

$$X=\omega\frac{\partial}{\partial x}+\mathrm{Re}\,\left(\lambda z+\tilde{B}(z,\bar{z},\sigma)+\varepsilon\tilde{F}(x,z,\bar{z},\sigma,\varepsilon)\right)\frac{\partial}{\partial z}\,,$$

where the dependence of $\tilde{B}$ and $\tilde{F}$ on B and F is straightforward. The tildes are dropped immediately.

The parametrised family of vector fields $X(\sigma,\varepsilon)$ can be viewed as a single *vertical* vector field X on the extended phase space

$$\mathcal{M}=\mathbb{T}^m\times\mathbb{R}^2\times P\times I,$$

where $I=(-\varepsilon_0,\varepsilon_0)$. The vector field X has vanishing components in the σ and ε directions; that is, if $\pi:\mathcal{M}\to P\times I$ is the canonical projection, the vector field X on $\mathcal{M}$ is vertical if $\pi_*X=0$. In the following, references to 'the' vector field X are usually held to be interchangeable with references to the family $X(\sigma,\varepsilon)$; from the context it should always be clear what is meant.

Normal form. By a standard normal form transformation $\psi = \psi(z, \bar{z}, \sigma)$, the vector field

$$Z = \mathrm{Re}\,\Big(\lambda z + B(z,\bar{z},\sigma)\Big)\frac{\partial}{\partial z} = \mathrm{Re}\,\Big(\mathrm{i}\alpha_0 z + (\lambda - \mathrm{i}\alpha_0)z + B(z,\bar{z},\sigma)\Big)\frac{\partial}{\partial z}$$

can be brought into normal form:

$$Z_{NF} = \mathrm{Re}\,\left(\mathrm{i}\alpha_0 z + g(|z|^2,\sigma)z + r(z,\bar{z},\sigma)\right)\frac{\partial}{\partial z},$$

where $g(|z|^2,\sigma) = \lambda - \mathrm{i}\alpha_0 + c(\sigma)|z|^2 + \mathsf{O}(|z|^4)$ and $r = \mathsf{O}(|z|^M)$, with M arbitrarily large. By a linear scaling of the variable z, it can moreover be achieved that the third order coefficient $c(\sigma)$ has absolute value 1; it will be replaced by $\mathrm{e}^{\mathrm{i}\vartheta(\sigma)}$ in the following. Assuming non-degenerateness of the dependence of ϑ on its argument, after a transformation the parameter σ can be assumed to be of the form $\sigma = (\mu, \alpha, \vartheta, \cdots)$.

Consequently, the transformation $\Psi(x,z,\bar{z},\sigma,\varepsilon) = (x, \psi(z,\bar{z},\sigma), \varepsilon)$ puts X in the form

$$X = \omega\frac{\partial}{\partial x} + \mathrm{Re}\,\left(\mathrm{i}\alpha_0 z + g(|z|^2,\sigma) + r(z,\bar{z},\sigma) + \varepsilon f(x,z,\bar{z},\sigma,\varepsilon)\right)\frac{\partial}{\partial z}, \qquad (5)$$

where r and f are smooth functions and where $r = \mathsf{O}(|z|^M)$.

3. Resonant normal forms

If $\langle k,\omega\rangle + \ell\alpha_0 = 0$ for $k \in \mathbb{Z}^m$ and $\ell \in \mathbb{Z}$, we say that the vector field X given by (5) is at a normal-internal $k:\ell$ resonance at the torus $\mathcal{T} = \mathbb{T}^m \times \{0\}$; note that it is simultaneously at a $(-k):(-\ell)$ resonance, so we might as well assume that ℓ is positive. In this section, we derive a normal form of X in this case, by applying averaging and van der Pol transformations. Most details of these transformations are given in Appendix B.

For normal-internal $k:1$ and $k:2$ resonances ordinary KAM theory does not cover the question of persistence of the torus $\mathcal{T}$ for small values of the perturbation strength $\varepsilon > 0$, basically because linearisation around $(z,\varepsilon) = (0,0)$ does not capture the approximate locus of the perturbed torus well enough. By first bringing the system into normal form, we shall see that the loci of the perturbed tori can approximately be described as the Cartesian product of a standard m-torus with the equilibria of a simple nonlinear planar vector field.

We briefly remark that a system in $k:\ell$ resonance cannot be in $\tilde{k}:\ell$ resonance if $\tilde{k} \neq k$. This follows from relation (4), since

$$\begin{aligned} 0 &= \left|\left\langle \tilde{k},\omega\right\rangle + \ell\alpha_0\right| = \left|\left\langle \tilde{k},\omega\right\rangle + \ell\alpha_0 - \langle k,\omega\rangle - \ell\alpha_0\right| = \left|\left\langle \tilde{k}-k,\omega\right\rangle\right| \\ &\geq \gamma|k-\tilde{k}|^{-\tau} > 0 \end{aligned}$$

is impossible.

Averaging. Let $\langle k,\omega\rangle+\ell\alpha_0=0$ for either $\ell=1$ or $\ell=2$. For λ close to $\mathrm{i}\alpha_0$, performing successive 'normal form' or 'averaging' transformations (see e.g. [11, 6, 45]) yields a coordinate system relative to which the vector field X is of the form

$$X=\omega\frac{\partial}{\partial x}+\mathrm{Re}\,\left(\mathrm{i}\alpha_0 z+g(|z|^2,\sigma)z+\varepsilon A\,\mathrm{e}^{\mathrm{i}\langle k,x\rangle}\bar{z}^{\ell-1}+r+\varepsilon R\right)\frac{\partial}{\partial z},$$

where $r=\mathsf{O}(|z|^M)$, $R=\mathsf{O}(|z|^2,\varepsilon)$ and, as before, $g(|z|^2,\sigma)=(\lambda-\mathrm{i}\alpha_0)+\mathrm{e}^{\mathrm{i}\vartheta}|z|^2+\mathsf{O}(|z|^4)$. Details of this transformation are given in Appendix B; there a more general form of the normal form system is derived. In the following, for several scalings the non-degeneracy condition $A\neq 0$ will be assumed to hold. Note that this is an open and dense condition on the set of vector fields X under study. After a trivial rescaling of the perturbation strength ε, we can assume that $A=1$.

Van der Pol transformation. The dependence on the torus coordinate x of terms of lowest order in z is removed by a van der Pol transformation, commonly called 'putting the system into co-rotating coordinates' (see e.g. [9, 16, 36, 39, 51]). Again, full details of this are given in Appendix B, but the idea is illustrated here for $\ell=1$ with the averaged form of X obtained in the previous paragraph. We perform the coordinate change $(x,z,\bar{z},\sigma,\varepsilon)\mapsto(x,\,\mathrm{e}^{-\mathrm{i}\langle k,x\rangle}z,\,\mathrm{e}^{\mathrm{i}\langle k,x\rangle},\sigma,\varepsilon)$. Recalling that we have $A=1$, this yields

$$X=\omega\frac{\partial}{\partial\tilde{x}}+\mathrm{Re}\,\left(g(|z|^2,\sigma)z+\varepsilon+\tilde{r}+\varepsilon\tilde{R}\right)\frac{\partial}{\partial z}\,,$$

where $g(|z|^2,\sigma)=(\lambda-\mathrm{i}\alpha_0)+\mathrm{e}^{\mathrm{i}\vartheta}|z|^2+\mathsf{O}(|z|^4)$, $\tilde{r}=\mathsf{O}(|z|^M)$ and $\tilde{R}=\mathsf{O}(|z|^2,\varepsilon)$.

The added difficulties in the general case come from the fact that we have to lift the vector field to an ℓ-fold covering space of the phase space. We show in Appendix B that the lifted vector field is of the form

$$X=\tilde{\omega}\frac{\partial}{\partial x}+\mathrm{Re}\,\Big(g(|z|^2,\sigma)z+\varepsilon\bar{z}^{\ell-1}+R_1(z,\bar{z},\sigma,\varepsilon)+\varepsilon R_2(x,z,\bar{z},\sigma,\varepsilon)\Big)\frac{\partial}{\partial z},$$

with g as above, $\tilde{\omega}$ again satisfying a Diophantine condition, $R_1=\mathsf{O}(\varepsilon|z|^{\ell+1},|z|^M)$ and $R_2=\mathsf{O}(|z|^N)$. We shall drop the tilde on $\tilde{\omega}$ in the following.

Rescaling. Next, we perform a rescaling of phase space at $\mathcal{T}$ and parameter space at $\lambda=\mathrm{i}\alpha_0$ respectively. Fix an open neighbourhood $\mathbb{T}^m\times U$ of $\mathbb{T}^m\times\{0\}$ by setting, e.g., $U=\{z\in\mathbb{C}\,:\,|z|<4\}$, and a compact neighbourhood K of 0 in parameter space by, e.g., $K=\{(\lambda,\vartheta)\in\mathbb{C}\times S^1\,:\,|\lambda|\leq 10\}$. These choices are made such that for all $\sigma\in K$, all equilibria of the scaled vector field to be introduced are in U.

For $\ell=1,2$ (or $\ell=3$) we perform the scaling

$$(x,z,\bar{z},\lambda,\vartheta,\varepsilon)\mapsto(x,\varepsilon^{-\frac{1}{4-\ell}}z,\varepsilon^{-\frac{1}{4-\ell}}\bar{z},\varepsilon^{-\frac{2}{4-\ell}}(\mathrm{i}\alpha_0-\lambda),\vartheta,\varepsilon),$$

and set $\varepsilon=\delta^{4-\ell}$ afterwards. The vector field X takes the form

$$X=\omega\frac{\partial}{\partial x}+\delta^2\,\mathrm{Re}\big(\lambda z+\,\mathrm{e}^{\mathrm{i}\vartheta}|z|^2z+\bar{z}^{\ell-1}\big)\frac{\partial}{\partial z}+\delta^3\tilde{Z}\,.$$

We put $Z_0 = \mathrm{Re}(\lambda z + \mathrm{e}^{\mathrm{i}\vartheta}|z|^2 z + \bar{z}^{\ell-1})\partial/\partial z$. From the more precise results derived in Appendix B it follows that X can actually be put in the form

$$X = \omega\frac{\partial}{\partial x} + \delta^2\left(Z_0 + \delta Z_1 + \delta^N Z_2\right), \tag{6}$$

where Z_1 is an integrable vector field, and where N can be choosen arbitrarily large.

Recall that the normal form vector field

$$\mathrm{Re}\left(\lambda z + c|z|^2 z + \bar{z}^{\ell-1}\right)\frac{\partial}{\partial z} \tag{7}$$

appears in the local analysis of $\ell:1$ resonances for $\ell \geq 3$ (see [1]). The present semi-global context motivates the study of this equation even for $\ell = 1$ and $\ell = 2$.

4. Bifurcation analysis of the $k:1$ resonance

In this section we perform a bifurcation analysis of the vector field Z_0 (given again in (7)) for $\ell = 1$. The analysis is complete with respect to local bifurcations, which are obtained analytically, and fairly comprehensive with respect to global bifurcations, which are obtained by numerical packages (AUTO, Matlab).

We consider

$$Z_0 = \mathrm{Re}\ \left(\lambda z + \mathrm{e}^{\mathrm{i}\vartheta}|z|^2 z + 1\right)\frac{\partial}{\partial z}\ ; \tag{8}$$

here $\lambda = \mu + \mathrm{i}\alpha$. This is a three-parameter family of planar vector fields, parametrised by (μ, α, ϑ); we shall see that the bifurcation diagram of this family has codimension 3 singularities of nilpotent-elliptic type as organising centres. Observe that Z_0 is symmetric with respect to the group generated by the involutions

$$(t, z, \lambda, \vartheta) \mapsto (t, \bar{z}, \bar{\lambda}, -\vartheta) \qquad \text{and} \qquad (t, z, \lambda, \vartheta) \mapsto (-t, -z, -\lambda, \vartheta + \pi).$$

Because of this symmetry, we can restrict our attention to the part of parameter space for which $0 \leq \vartheta \leq \pi/2$; in this restricted parameter space, there is exactly one singularity of nilpotent-elliptic type.

Figure 1 gives a graphical overview of our results on the position of the bifurcation manifolds that correspond to local bifurcations of codimension 1 and 2. The codimension 2 bifurcation curves corresponding to cusp and Bogdanov-Takens bifurcations are indicated in figure 1-(a). Figure 1-(b) shows the relative positions of the codimension 1 bifurcation manifolds in the vicinity of a singularity of nilpotent-elliptic type.

Codimension 1 bifurcations. The codimension 1 bifurcation manifolds of Z_0 have been determined in [53]. We summarise the result in the following proposition.

Proposition 1. *Let the family of complex differential equations*

$$\dot{z} = (\mu + \mathrm{i}\alpha)z + \mathrm{e}^{\mathrm{i}\vartheta}|z|^2 z + 1$$

be given. The local bifurcations of codimension 1 of this family determine the following bifurcation manifolds.

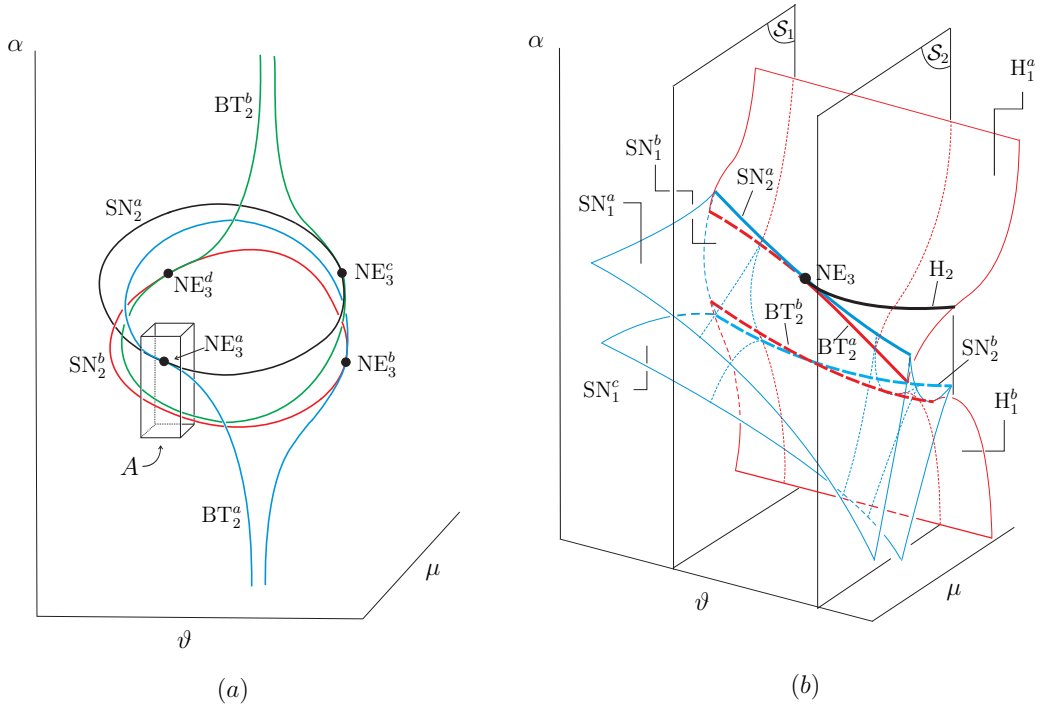


Figure 1. (a): Sketch of the global bifurcation diagram of $\dot{z} = (\mu + i\alpha)z + \mathrm{e}^{i\vartheta}|z|^2 z + 1$ in the (ϑ, μ, α)-parameter space. All singularity of nilpotent-elliptic points (NE_3) are connected by cusp (SN_2) and Bogdanov-Takens (BT_2) lines. The curves BT_2^a and BT_2^b tend to $\pm\infty$, respectively, when ϑ goes to $\pi/2$. (b): Detail of the bifurcation set in box A of figure (a). At the singularity of nilpotent-elliptic type (NE_3) point, curves of Bogdanov-Takens (BT_2^a), cusp (SN_2^a), and degenerate Hopf (H_2) bifurcations meet tangently. The curves BT_2^b and SN_2^b do not intersect. For terminology see table A1

(i) A saddle-node bifurcation surface SN_1*, given by*

$$s(\rho) = \rho_1^4\rho_2^2 + 2\rho_1^2\rho_2^4 + \rho_2^6 + \rho_1^3 + 9\rho_1\rho_2^2 + \frac{27}{4} = 0, \qquad \operatorname{grad} s(\rho) \neq 0, \tag{9}$$

where $\rho_1 = \mu\cos\vartheta + \alpha\sin\vartheta$ *and* $\rho_2 = \alpha\cos\vartheta - \mu\sin\vartheta$.

(ii) A Hopf bifurcation surface H_1*, given by*

$$\mu^3 - 4\mu^2\alpha\cos\vartheta\sin\vartheta + 4\mu\alpha^2\cos^2\vartheta + 8\cos^3\vartheta = 0, \tag{10}$$

$$(\alpha - \mu\tan\vartheta)^2 - \left(\frac{\mu}{2\cos\vartheta}\right)^2 > 0. \tag{11}$$

Not all points on H_1 *correspond to non-degenerate Hopf bifurcation points.*

See [53] for the proof of this proposition. We will show below that there is a curve H_2 of degenerate Hopf bifurcation points on the manifold H_1, such that all points in $\mathrm{H}_1 \backslash \mathrm{H}_2$ are nondegenerate Hopf bifurcation points. The results of the proposition are illustrated by the bifurcation diagrams in figure 2.

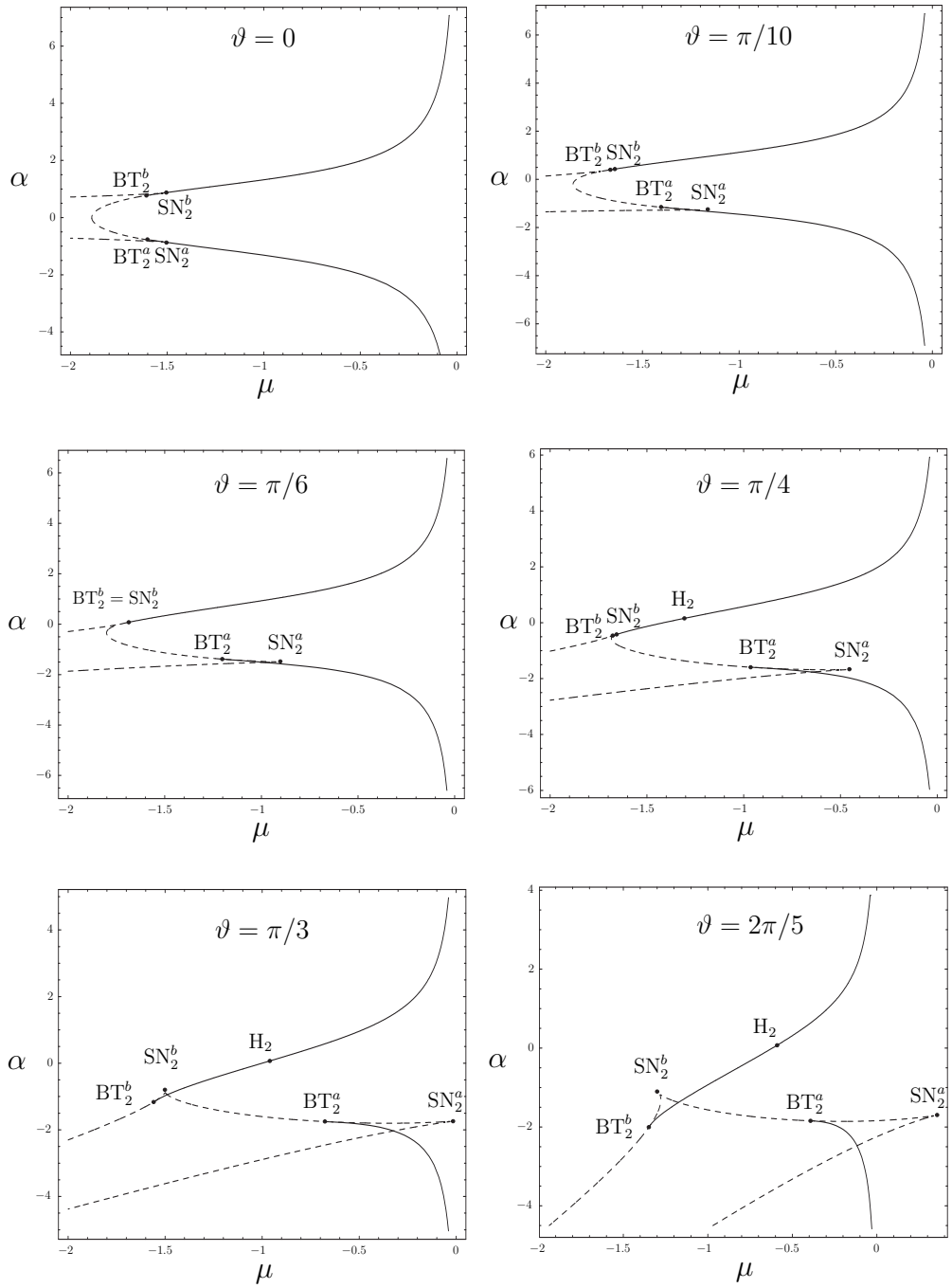


Figure 2. Bifurcation diagram of $\dot{z} = (\mu + i\alpha)z + \mathrm{e}^{i\vartheta}|z|^2 z + 1$ for fixed values of ϑ in the (μ, α)-plane. Solid curves indicate Hopf bifurcations, dashed curves indicate saddle-node bifurcations. For $\vartheta = \pi/6$, the BT_2, SN_2 and H_2 points coalesce in a NE_3 bifurcation point. Note that all the bifurcation curves are intersections of the bifurcation manifolds of Figure 1-(b) with planes $\vartheta = const.$ In Figure 1-(b) two of these planes are indicated by $\mathcal{S}_1$ and $\mathcal{S}_2$. For terminology see table A1

Codimension 2 bifurcations. Next, we consider the manifolds of local codimension 2 bifurcations of the vector field Z_0 for $\ell = 1$: we find cusp (SN_2), Bogdanov-Takens (BT_2) and degenerate Hopf (H_2) bifurcation points. The cusp and Bogdanov-Takens bifurcations have already been given in [53]. We show here that the vector field Z_0 has also a curve of degenerate Hopf bifurcation points for $\pi/6 \le \vartheta < \pi/2$. These are the only local codimension 2 bifurcations of the system.

Proposition 2. *The local bifurcations of codimension 2 of the equilibria of the differential equation*

$$\dot z = (\mu + \mathrm{i}\alpha)z + \mathrm{e}^{\mathrm{i}\vartheta}|z|^2 z + 1 \tag{12}$$

are the following.

(i) There are two curves of cusp bifurcation points SN_2^a and SN_2^b. Two components of the manifold SN_1 of saddle node points meet tangently at these curves. The curves are given by

$$SN_2^a: \qquad \mu = -\frac{3}{2}\cos\vartheta + \frac{\sqrt{3}}{2}\sin\vartheta, \quad \alpha = -\frac{3}{2}\sin\vartheta - \frac{\sqrt{3}}{2}\cos\vartheta, \tag{13}$$

and by

$$SN_2^b: \qquad \mu = -\frac{3}{2}\cos\vartheta - \frac{\sqrt{3}}{2}\sin\vartheta, \quad \alpha = -\frac{3}{2}\sin\vartheta + \frac{\sqrt{3}}{2}\cos\vartheta. \tag{14}$$

(ii) The system has two Bogdanov-Takens curves BT_2^a and BT_2^b, where the saddle-node and Hopf surfaces meet tangently. The curves are given by

$$BT_1^a: \qquad \mu = \frac{-2\cos\vartheta}{(2\sin\vartheta+2)^{1/3}}, \quad \alpha = \frac{-2\sin\vartheta - 1}{(2\sin\vartheta+2)^{1/3}}, \tag{15}$$

and

$$BT_2^b: \qquad \mu = \frac{-2\cos\vartheta}{(2-2\sin\vartheta)^{1/3}}, \quad \alpha = \frac{-2\sin\vartheta + 1}{(2-2\sin\vartheta)^{1/3}}. \tag{16}$$

(iii) The system has a degenerate Hopf bifurcation curve H_2 given by

$$H_2: \qquad \mu = -2\cos\vartheta, \quad \alpha = 0, \quad \frac{\pi}{6} < \vartheta < \frac{\pi}{2}.$$

Proof.
The cusp and Bogdanov-Takens curves have been obtained in [53]. It remains to find the degenerate Hopf bifurcation points.

In real coordinates $y_1 = \mathrm{Re}\, z$ and $y_2 = \mathrm{Im}\, z$, equation (12) reads

$$\begin{aligned} \dot y_1 &= \mu y_1 - \alpha y_2 + (y_1^2 + y_2^2)(y_1\cos\vartheta - y_2\sin\vartheta) + 1, \\ \dot y_2 &= \alpha y_1 + \mu y_2 + (y_1^2 + y_2^2)(y_1\sin\vartheta + y_2\cos\vartheta). \end{aligned} \tag{17}$$

Let $y_0 = (y_{10}, y_{20})$ be an equilibrium of this system. Translating it to the origin by putting $(y_1, y_2) = (y_{10}, y_{20}) + (u, v)$ yields a system of the form

$$\begin{pmatrix} \dot{u} \\ \dot{v} \end{pmatrix} = \begin{pmatrix} a_1 & a_2 \\ b_1 & b_2 \end{pmatrix} \begin{pmatrix} u \\ v \end{pmatrix} + \begin{pmatrix} a_3u^2 + a_4uv + a_5v^2 \\ b_3u^2 + b_4uv + b_5v^2 \end{pmatrix} + \begin{pmatrix} a_6u^3 + a_7u^2v + a_6uv^2 + a_7v^3 \\ -a_7u^3 + a_6u^2v - a_7uv^2 + a_6v^3 \end{pmatrix}, \tag{18}$$

where all coefficients are functions of μ, α and ϑ; their precise form is given in Appendix C. At a Hopf bifurcation point, the eigenvalues $\lambda, \bar{\lambda}$ of the linear part of (18) are purely imaginary. Let

$$w = \frac{(\lambda - a_1)u - a_2 v}{\operatorname{Im} \lambda}.$$

Then we have

$$\begin{aligned} \dot{w} = {} & \lambda w + B_1 w^2 + B_2 w\bar{w} + B_3 \bar{w}^2 \\ & + B_4 w^3 + B_5 w^2 \bar{w} + B_6 w \bar{w}^2 + B_7 \bar{w}^3, \end{aligned} \tag{19}$$

where each B_i is a function of μ, α and ϑ; these functions are also given in Appendix C. Using standard normal form transformations, we can simplify equation (19) to obtain (see for instance [55, 6, 40])

$$\dot{w} = \lambda w + C_1(\mu, \alpha, \vartheta) w^2 \bar{w} + C_2(\mu, \alpha, \vartheta) w^3 \bar{w}^2 + \mathcal{O}(|w|^7), \tag{20}$$

where

$$C_1 = \frac{B_5}{2} + \frac{B_1 B_2 (2\lambda + \bar{\lambda})}{2|\lambda|^2} + \frac{|B_2|^2}{\lambda} + \frac{|B_3|^2}{2(2\lambda - \bar{\lambda})}.$$

Solving equation $\operatorname{Re}(C_1) = 0$, together with equation (10), yields the location of the degenerate Hopf points in the (μ, α)-plane

$$\mu = -2\cos\vartheta, \quad \alpha = 0. \tag{21}$$

For $\vartheta \in [0, \pi/6)$, inequality (11) is not satisfied; therefore degenerate Hopf bifurcations only occur for $\vartheta \in [\pi/6, \pi/2)$, compare figure 2.

The expression of $\operatorname{Re} C_2$ is quite complicated. It is given in Appendix C; there it is shown that $\operatorname{Re} C_2$ does not vanish at degenerate Hopf points, implying that the degenerate Hopf points are not doubly degenerate. ∎

Below we also show that the cusp and Bogdanov-Takens bifurcations are nondegenerate everywhere except at the nilpotent-elliptic point NE_3.

Singularity of nilpotent-elliptic type as organising centre. The bifurcation diagram of the family Z_0 possesses a singularity of nilpotent-elliptic type (see [25]), which acts as an organising centre of the three-dimensional bifurcation diagram.

Proposition 3. *The bifurcation set of Z_0 has a single singularity of nilpotent-elliptic type. This is the only local bifurcation point of codimension 3 of the family Z_0.*

Proof.
We use the same transformation to local coordinates around an equilibrium as in the beginning of the proof of proposition 2. On the Bogdanov-Takens curves, the system can be written as

$$\begin{aligned}\begin{pmatrix}\dot{y}_1\\ \dot{y}_2\end{pmatrix} &= \begin{pmatrix}0 & 1\\ 0 & 0\end{pmatrix}\begin{pmatrix}y_1\\ y_2\end{pmatrix} \\ &+ \begin{pmatrix}b_5b_1y_1^2 + b_4y_1y_2 + (b_3/b_1)y_2^2\\ a_5b_1^2y_1^2 + a_4b_1y_1y_2 + a_3y_2^2\end{pmatrix} \\ &+ \begin{pmatrix}a_6b_1^2y_1^3 - a_7b_1y_1^2y_2 + a_6y_1y_2^2 - (a_7/b_1)y_2^3\\ a_7b_1^3y_1^3 + a_6b_1^2y_1^2y_2 + a_7b_1y_1y_2^2 + a_6y_2^3\end{pmatrix}.\end{aligned} \tag{22}$$

Using a standard normal form procedure [48, 6], we find

$$\begin{aligned}\begin{pmatrix}\dot{y}_1\\ \dot{y}_2\end{pmatrix} &= \begin{pmatrix}0 & 1\\ 0 & 0\end{pmatrix}\begin{pmatrix}y_1\\ y_2\end{pmatrix} + \begin{pmatrix}0\\ K_1y_1^2 + K_2y_1y_2\end{pmatrix} \\ &+ \begin{pmatrix}0\\ K_3y_1^3 + K_4y_1^2y_2\end{pmatrix} + \begin{pmatrix}0\\ K_5y_1^4 + K_6y_1^3y_2\end{pmatrix}\end{aligned} \tag{23}$$

where for $i = 1, 2, \cdots, 6$, the coefficient K_i is a function of μ, α and ϑ. All coefficients are specified in Appendix C.
Solving equation $K_1 = 0$ on the Bogdanov-Takens lines, gives the location of singularities of nilpotent-elliptic type (NE_3) bifurcation point in (μ, α, ϑ)-space [25]. The NE_3 point occurs at

$$(\mu, \alpha, \vartheta) = (-\sqrt{3}, 0, \pi/6).$$

At this point, the 4-jet of vector field (23) is C^∞-conjugate to

$$\begin{aligned}\dot{y}_1 &= y_2\\ \dot{y}_2 &= -y_1^3 + 2\sqrt{3}y_1y_2 + \sqrt{3}y_1^2y_2 + 4y_1^4 - \tfrac{65}{12}\sqrt{3}y_1^3y_2,\end{aligned} \tag{24}$$

see [25, 48]. The coefficient of the term y_1y_2 is larger than $2\sqrt{2}$, and the coefficient of the term y_1^3 is -1. This implies that the singularity is of 'nilpotent-elliptic' type (see [25] for the nomenclature).

A simple computation shows that neither degenerate cusp nor double degenerate Hopf bifurcations occur in the present model. ∎

Phase portraits. In this section, we extend the description of the bifurcation diagram of equation (8) given in [53]. In figure 3, we plot the two-dimensional bifurcation diagram of system (8) for the two planes $\vartheta = 2\pi/5$ and $\vartheta = \pi/10$ respectively. Figure 4 gives the phase portraits of the system for parameters in different regions of the bifurcation diagrams. Phase portraits are plotted using Matlab [31].

We find all local bifurcations of (8): saddle-node (SN_1), Hopf (H_1), cusp (SN_2), Bogdanov-Takens (BT_2) and degenerate Hopf (H_2) bifurcations, which are expected

from the bifurcation diagram of a singularity of nilpotent-elliptic type [25]. We also retrieve homoclinic and saddle-node of limit cycles bifurcations; these are found using the numerical packages Auto [22] and Matlab [31, 28] respectively. These bifurcations are drawn in figure A2.

We do not recover the following bifurcations whose existence is also predicted by [25]: cycle tangency (CT_1), double tangency (DT_1), separatrix tangency (ST_1), double cycle tangency (DCT_2), double centre separatrix tangency ($DCST_2$) and hyperbolic separatrix tangency bifurcations.

Remark. System (8) also contains a global feature, namely, a large homoclinic loop of a hyperbolic saddle point, which is not explained by the nilpotent-elliptic singularity. This large homoclinic loop is detected by Auto [22]. See figure 4.

5. Bifurcation analysis of the $k:2$ resonance

We continue by performing a bifurcation analysis of the vector field Z_0 for the case $\ell = 2$. As remarked before, in this case it is sufficient to consider two bifurcation parameters. The local bifurcations in the $\ell = 2$ case have already been given in [27, 53]; in this section, after briefly recalling those results, global bifurcations are determined numerically whose existence follow from our knowledge of the local bifurcation diagram. The results of this section are echoed in [41]; see also [50].

We consider the principal part vector field

$$Z_0 = \mathrm{Re}\,\left(\lambda z + \mathrm{e}^{\mathrm{i}\vartheta}|z|^2 z + \bar{z}\right)\frac{\partial}{\partial z}\,. \tag{25}$$

This is a two-parameter family of planar vector fields as we shall treat in this section ϑ as a generic constant. Observe that Z_0 is symmetric with respect to the group generated by the two involutions

$$(z,\lambda,\vartheta)\mapsto(\bar{z},\bar{\lambda},-\vartheta) \qquad \text{and} \qquad (z,\lambda,\vartheta)\mapsto(-z,\lambda,\vartheta).$$

Because of this symmetry, we can restrict our attention to those values of ϑ satisfying $0 \le \vartheta \le \pi$.

Local bifurcations. For the determination of the local bifurcations of codimension 1 and 2, see [53]. We summarise the result.

Proposition 4. *Let the family of complex differential equation*

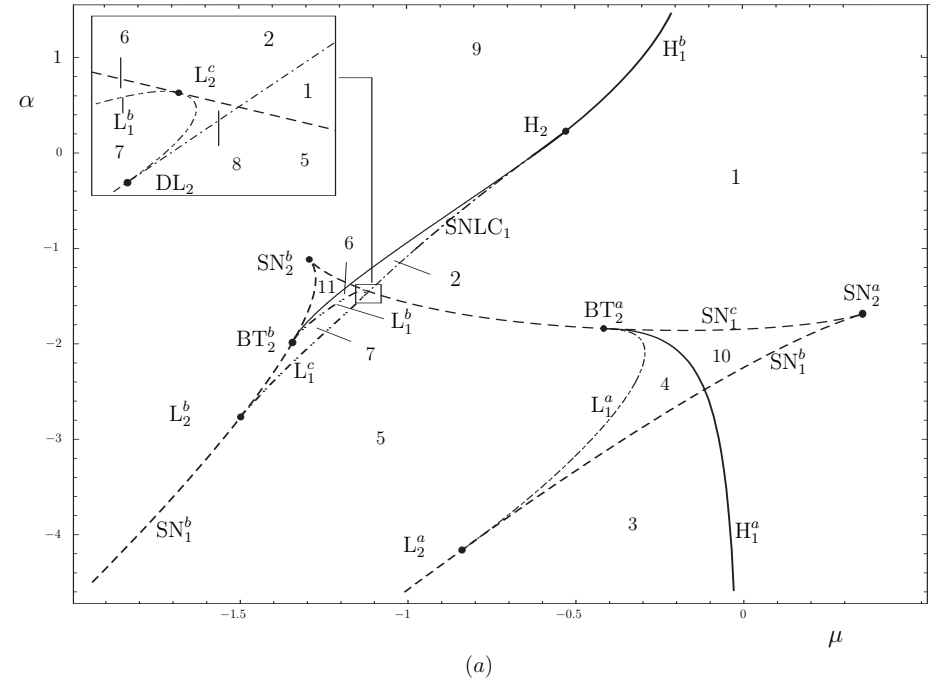
$$\dot{z} = (\mu + \mathrm{i}\alpha)z + \mathrm{e}^{\mathrm{i}\vartheta}|z|^2 z + \bar{z}$$

be given. Set $\rho_1 = \mu\cos\vartheta + \alpha\sin\vartheta$, $\rho_2 = \alpha\cos\vartheta - \mu\sin\vartheta$ and $\rho = \rho_1 + \mathrm{i}\rho_2$.

Then the local bifurcations of codimension 1 of this family determine the following bifurcation manifolds.

(i) A curve of pitchfork bifurcations PF_1

$$|\rho| = 1. \tag{26}$$



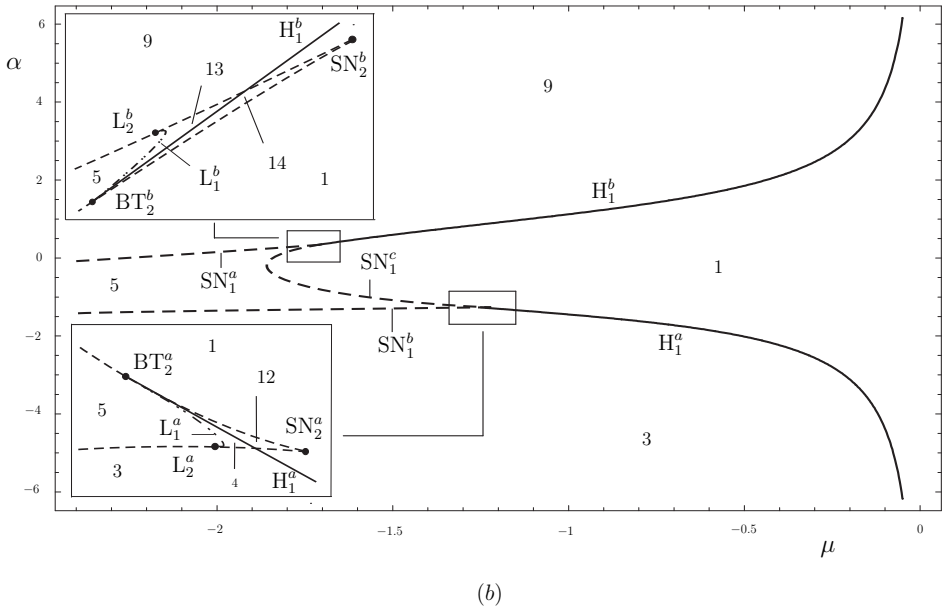


Figure 3. Two-dimensional bifurcation diagrams of system (8). (*a*): For $\vartheta = 2\pi/5$. (*b*): For $\vartheta = \pi/10$. Phase portraits for every region are given in Figure 4. For terminology see table A1

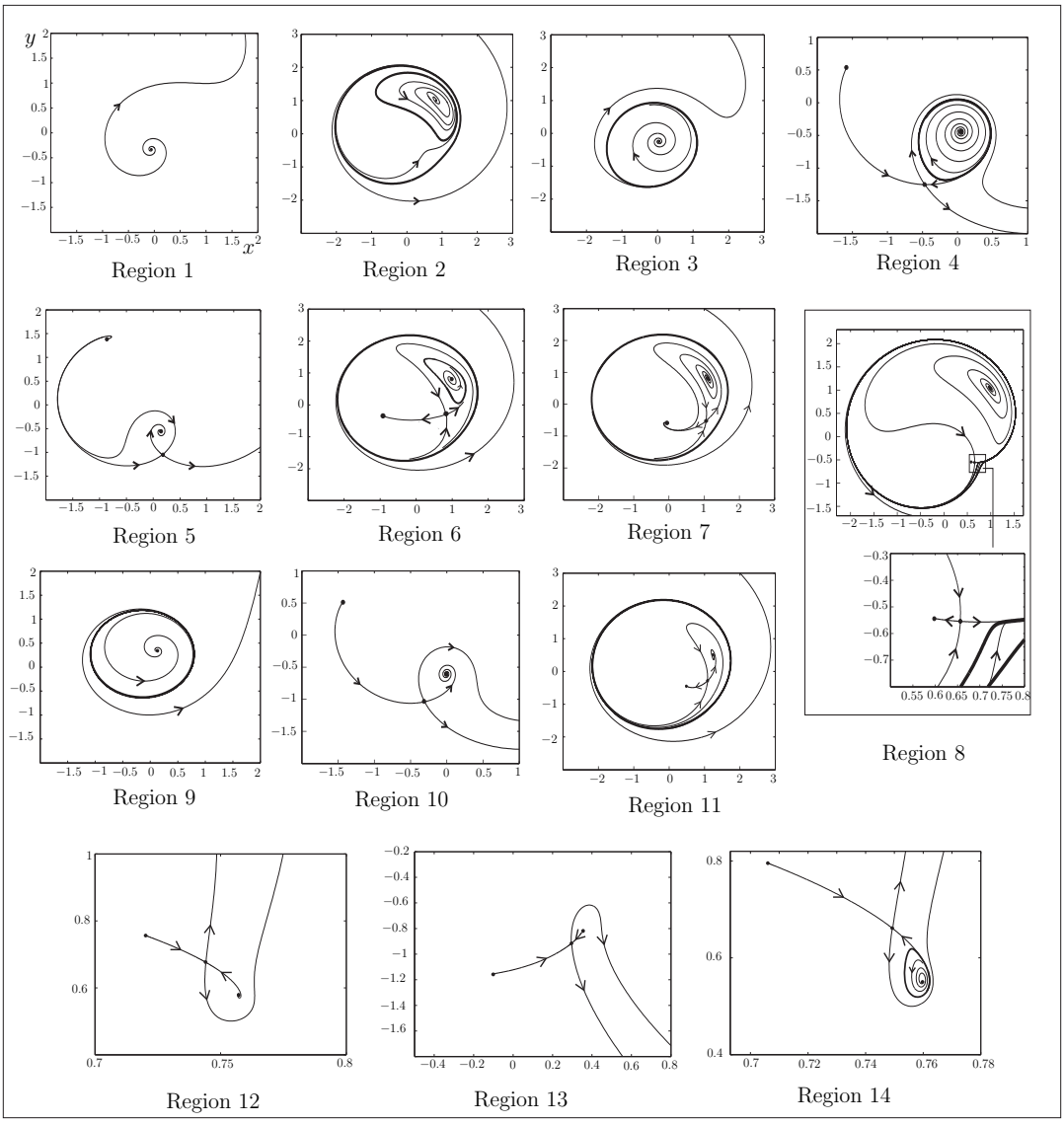


Figure 4. Generic phase portraits of the family (8) for parameters in the different regions of the bifurcation diagrams in Figure 3. For regions 1, 2, 3 and 9, single orbits, leaving an unstable equilibrium or unstable periodic orbits are shown. For all other regions, stable and unstable manifolds of saddle points are drawn.

(ii) Two curves of saddle-node bifurcations SN_1, given by

$$\rho_2^2 = 1, \qquad \rho_1 < 0. \tag{27}$$

(iii) Three Hopf bifurcation H_1 curves; two are given by

$$\mathrm{Re}\,(\,\mathrm{e}^{\mathrm{i}\vartheta}\rho) = 0, \qquad |\rho| > 1, \tag{28}$$

and the third by

$$\begin{aligned} &\frac{1}{4}(\rho_1 + \rho_2 \tan\vartheta)^2 + \rho_2^2 = 1, \\ &\frac{1}{2}\rho_1^2 + \frac{\tan\vartheta}{2}\rho_1\rho_2 + \rho_2^2 < 1, \quad \rho_2 \tan\vartheta - \rho_1 > 0. \end{aligned} \tag{29}$$

The local codimension 2 bifurcations correspond to the following bifurcation points.

(i) Two degenerate pitchfork bifurcation PF_2 points at

$$\rho = \mathrm{i} \quad \textit{and} \quad \rho = -\mathrm{i}. \tag{30}$$

(ii) Two symmetric double-zero bifurcations SDZ_2 at

$$\lambda = \mathrm{i} \quad \textit{and} \quad \lambda = -\mathrm{i}. \tag{31}$$

(iii) A Bogdanov-Takens bifurcation point BT_2 at

$$\rho = |\tan\vartheta| \left(1 + \frac{\mathrm{i}}{\tan\vartheta}\right). \tag{32}$$

The local bifurcations described by this proposition are shown in figure 5. Moreover, from the occurrence of a Bogdanov-Takens bifurcation, we infer the existence of a homoclinic bifurcation curve L_1. One of the symmetric double zero SDZ_2 bifurcation points gives rise to curves of saddle-nodes of limit cycles SNLC_1, Hopf bifurcations H_1 and homoclinic loops L_1. This last curve ends on the curve of pitchfork bifurcation PF_1; at that point, a curve of heteroclinic bifurcation points He_1 departs that ends on a line of saddle-nodes of equilibria SN_1. At the other SDZ_2 point, we have a second curve of heteroclinic bifurcations He_1, also ending on a saddle-node line. These lines are given in the bifurcation diagram in figure 5.

6. Persistence of the bifurcation diagram

In section 2, a normal form of the vector field X at a resonance $\langle k, \omega\rangle + \alpha_0 = 0$ has been obtained (equation (6)). Rescaling time by $t \mapsto \delta^{-2}t$ changes X to

$$X = \delta^{-2}\omega\frac{\partial}{\partial x} + Z_0 + \delta Z_1 + \delta^N Z_2. \tag{33}$$

In sections 4 and 5, local bifurcation diagrams have been given for the integrable family

$$Z_0 = \mathrm{Re}\,\left(\lambda z + \mathrm{e}^{\mathrm{i}\vartheta}|z|^2 z + \bar{z}^{\ell-1}\right)\frac{\partial}{\partial z}$$

for $\ell = 1$ and $\ell = 2$ respectively. This section investigates the bifurcation diagrams of the full family X for small values of δ, by successively adding the perturbation terms δZ_1 and $\delta^N Z_2$ to the integrable vector field $\delta^{-2}\omega\frac{\partial}{\partial x} + Z_0$.

The bifurcation analysis is performed for (z, σ) in the compact closure of some bounded open neighbourhood $U \times \Sigma$ of $(0, 0)$ in $\mathbb{C} \times \mathbb{R}^q$. Since z and σ are not required to be small, while δ is taken close to 0, this is called *semi-global bifurcation analysis*.

6.1. Persistence under integrable perturbations

Recall the definitions of $K = \{\lambda \in \mathbb{C} : |\lambda| \leq 10\}$ and $U = \{z \in \mathbb{C} : |z| < 4\}$ from section 3. We have seen there that for $(\lambda, \vartheta) \in K$ all equilibria of the vector field Z_0 are in the interior of U. There is a $\delta_0 > 0$ such that for $|\delta| < \delta_0$, the local parts of the

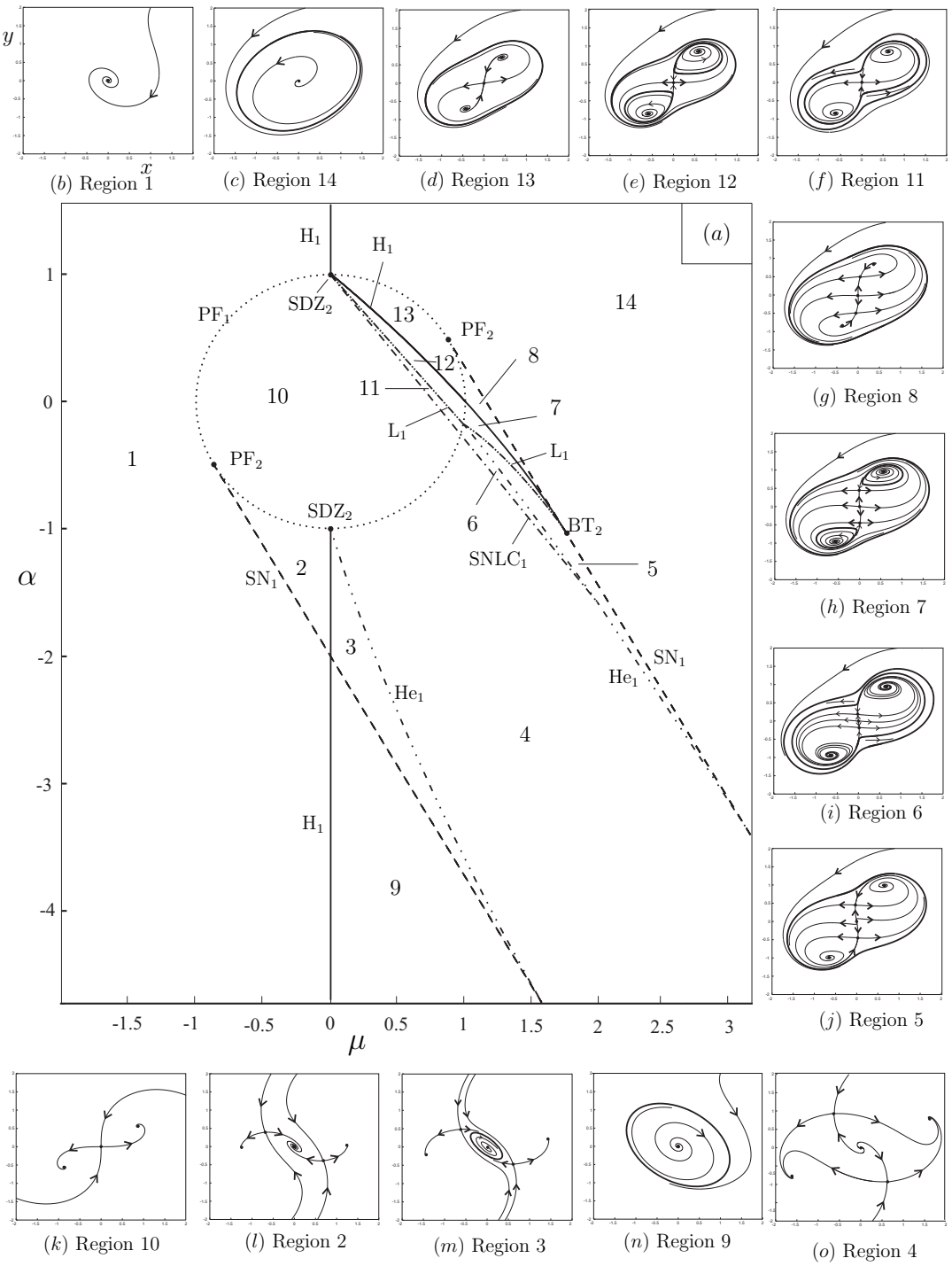


Figure 5. (a): Bifurcation diagram of system (25), for $\vartheta = 2\pi/3$. $(b) - (o)$: Generic phase portraits for different regions in the parameter space. For the terminology see table A1

bifurcation diagrams of Z_0 and $Z_0 + \delta Z_1$ restricted to U are equal, modulo at most a change of coordinates, since all local bifurcations singularities obtained have been shown to be nondegenerate.

Indeed, all singularities can be continued as a function of δ over some interval $\Delta_{(\lambda,\vartheta)}$; since (λ, ϑ) take values in the compact set K, there is a constant $\delta_0 > 0$ such that $[-\delta_0, \delta_0] \subset \Delta_{(\lambda,\vartheta)}$ for all $(\lambda, \vartheta) \in K$. The parametrisation furnishes us an invertible correspondence between the bifurcation diagrams.

6.2. Persistence under non–integrable perturbations

A more intricate issue is persistence of bifurcations in the family $Z_0 + \delta Z_1$ under non-autonomous (quasi-periodic) perturbations $\delta^N Z_2$; or, put differently, which bifurcations of m-dimensional tori in the integrable family $X_1 = Z_0 + \delta Z_1$ persist quasi-periodic bifurcations in $X = Z_0 + \delta Z_1 + \delta^N Z_2$?

We have to invoke quasi-periodic bifurcation theory, as introduced in [11]. This area is under active development (see for instance [9, 52, 30, 54]); in the sequel some results will therefore be formulated as conjectures. Note however that the present set-up is simpler that the usual one, since the dynamics on the torus are not perturbed. This is analogous to the situation considered in [9].

Quasi–periodic saddle node and cusp bifurcations. Take a point σ_0 on a saddle-node manifold of $X_1 = Z_0 + \delta Z_1$. A suitable change of the normal coordinate Φ brings the system locally into saddle-node normal form

$$\Phi_* X_1 = \tfrac{1}{\delta^2}\omega \frac{\partial}{\partial x} + \left(\eta(\sigma) + a_2(\sigma, w)w^2\right) \frac{\partial}{\partial w} + b_1(\sigma, y) y \frac{\partial}{\partial y};$$

here $x \in \mathbb{T}^m$, $w, y \in \mathbb{R}$ and $a_2(\sigma_0, 0) \neq 0 \neq b_1(\sigma_0, 0)$. Since σ_0 is a non-degenerate saddle-node point, we have that $\eta(\sigma_0) = 0$, and $\frac{\mathrm{d}\eta}{\mathrm{d}\sigma}(\sigma_0) \neq 0$. Applying the transformation Φ to the vector field X instead of X_1 yields

$$\begin{aligned}\Phi_* X = \tfrac{1}{\delta^2}\omega \frac{\partial}{\partial x} \\ + \left(\eta(\sigma) + a_2(\sigma, w)w^2 + \delta^N r_1\right) \frac{\partial}{\partial w} + \left(b_1(\sigma, y)y + \delta^N r_2\right) \frac{\partial}{\partial y},\end{aligned}$$

where the functions r_1 and r_2 depend smoothly on $(x, w, y, \sigma, \delta)$.

Since ω is Diophantine, $\delta^{-2}\omega$ is Diophantine as well, and if $\delta > 0$ is sufficiently small, it follows from the theory in [11] or [52] that by a smooth near-identity transform, the vector field $\Phi_* X$ can be transformed to

$$\tilde{X} = \tfrac{1}{\delta^2}\omega \frac{\partial}{\partial x} + \left(\tilde{\eta} + \tilde{a}_2(\tilde{\sigma}, w)w^2\right) \frac{\partial}{\partial w} + \tilde{b}_1(\tilde{\sigma}, y) y \frac{\partial}{\partial y},$$

such that $\tilde{\sigma} = (\eta, \cdots)$, $\tilde{a}_2(0, 0) \neq 0$ and $\tilde{b}_1(0, 0) \neq 0$. This can be accomplished by a smooth transformation, C^r-δ^N close to the identity for every r. Hence quasi-periodic saddle-node bifurcations persist locally.

From the results in [52] it follows that in the same manner, quasi-periodic cups bifurcations persist in the family X, if $\delta > 0$ is sufficiently small.

Quasi-periodic Hopf bifurcations In the case of Hopf bifurcations, the situation is different because of possible resonances of $\delta^{-2}\omega$ with the normal frequency.

Similarly as in the case of the saddle-node and cusp bifurcations, for a parameter $\sigma_0 = (\lambda_0, \cdots)$ on a Hopf bifurcation manifold of X_1 the vector field X can be brought in the form

$$\Phi_* X = \tfrac{1}{\delta^2}\omega \frac{\partial}{\partial x} + \left(\lambda z + b_3(\sigma)|z|^2 z + \mathsf{O}(\delta^N, |z|^5)\right) \frac{\partial}{\partial z},$$

with $\lambda_0 = \mathrm{i}\alpha_0$, $\alpha_0 > 0$.

Define the sets

$$D_n(\gamma,\tau) = \Big\{\lambda \in \mathbb{C} \,:\, |\ell\lambda + \mathrm{i}\langle k,\omega\rangle| \geq \gamma(|k|+|\ell|)^{-\tau}, \\ \forall (k,\ell) \in \mathbb{Z}^m \times \mathbb{Z},\ 0 < |\ell| \leq n\Big\}.$$

If $V \subset X$ is a set in the space X, let $\complement V$ denote the complement $X \backslash V$ of V in X. For $\tau > m-1$ and $U \subset \mathbb{C}$ an open set, we have that $C_\gamma = \complement\,(U \cap D_n(\gamma,\tau))$ satisfies

$$\text{meas } C_\gamma = \mathsf{O}(\gamma),$$

where ' meas ' denotes Lebesgue measure (see e.g. [11]). Then it follows from the results of in [3, 11] that for small enough δ, the vector field X can be transformed into

$$\tilde{X} = \tfrac{1}{\delta^2}\omega \frac{\partial}{\partial x} + \left(\tilde{\lambda} z + \tilde{b}_3(\tilde{\sigma})|z|^2 z + r(x,z,\bar{z},\tilde{\sigma}) + \mathsf{O}(|z|^5)\right) \frac{\partial}{\partial z},$$

where r, together with all its derivatives, vanishes if $(\omega,\tilde{\lambda}) \in D_4(\delta^{N+1},\tau)$.

Those parameters that satisfy $\operatorname{Re}\tilde{\lambda} = 0$ are quasi-periodic Hopf bifurcation parameters for the invariant m-dimensional torus $z = 0$ of $\tilde{X}$. There is a C^∞ curve $\mathcal{H}$, C^r-δ^N close to the curve H of Hopf bifurcations in the bifurcation diagram of $Z_0 + \delta Z_1$, and a nowhere dense subset $\mathcal{H}_c$ on $\mathcal{H}$, such that

$$\mu(\mathcal{H} \backslash \mathcal{H}_c) \leq c\delta^{N+1}$$

and all points of $\mathcal{H}_c$ are non-degenerate quasi-periodic Hopf bifurcation points of the family $\tilde{X}$.

Other quasi-periodic bifurcations. The previous two cases are typical. Let us go over the cases of higher codimension a little more quickly. The general type of result is however always the same: if at a certain singularity the normal frequencies are fixed to a particular value, as it is for instance the case in the Bogdanov-Takens bifurcation, then the corresponding bifurcation curve persists in its entirety, whereas if they only have to satisfy a non-resonance condition, then only a large measure subset of the bifurcation curve persists under perturbation.

In particular the methods developed in [54] imply that the Bogdanov-Takens points and the singularities of nilpotent-elliptic type persist in their entirety. It is a corollary of the results in [52], generalising [19], that a large measure subset of the degenerate Hopf bifurcation curve persists (see also [14]). For global bifurcations like homoclinic loops, we again refer to [14] where a methodological framework is developed to study these bifurcations.

Semi-global quasi-periodic bifurcation diagram. Patching up the local results as in the previous subsection, the local bifurcation diagram of $Z_0+\delta Z_1$ persists as a quasi-periodic local bifurcation diagram under a small perturbation, except for a set of measure less than $c\delta^{N+1}$ on the quasi-periodic Hopf and degenerate Hopf bifurcation curves.

6.3. Resonances within resonances

At the end of the previous subsection, a subset H_c of large measure of the Hopf bifurcation curve H of the integrable family

$$X_1 = \left(\ell\delta^2\right)^{-1}\omega\frac{\partial}{\partial x} + Z_0 + \delta Z_1,$$

was shown to persist as $\mathcal{H}_c$ if a non-integrable term $\delta^N Z_2$ was added. In the complement of H_c in H are $k:\ell$ resonance points with $\ell \in \{1,2,3,4\}$. Leaving aside $k:3$ and $k:4$ resonances, we note that the analysis of the present paper can be reapplied to the case of $k:1$ and $k:2$ resonances.

Let λ_0 be a point on a Hopf bifurcation curve of X_1, such that the normal frequency α_0 of the bifurcating torus $z=z_0$ is in $k:1$ resonance at λ_0. In suitable local coordinates (z,λ) around (z_0,λ_0), the vector field X takes the form:

$$X = \delta^{-2}\omega\frac{\partial}{\partial x} + \left(\lambda z + c|z|^2 z + R\right)\frac{\partial}{\partial z}, \tag{34}$$

where $R = \mathsf{O}(|z|^5, \delta^N)$.

It is not *a priori* obvious whether the appropriate non-degeneracy condition is satisfied (see section 3). However, if a term

$$\delta^N \kappa\, \mathrm{e}^{\mathrm{i}\langle k,x\rangle}\frac{\partial}{\partial z},$$

is added to the original vector field (3) (or to (34), which amounts to the same), inspection of the transformations in Appendix B shows that the final vector field will be changed by an amount

$$\delta^N \kappa\, \mathrm{e}^{\mathrm{i}\langle k,x\rangle}\frac{\partial}{\partial z} + \mathsf{O}(\delta^{N+1}),$$

at its worst. Hence, after choosing κ appropriately, the non-degeneracy condition may be assumed to hold.

Hence, for an open and dense set of perturbations, the analysis performed in this paper can be iterated finitely many times, yielding a constant $\tilde{\delta}_0$ such that for $|\delta| \le \delta_0$, the Hopf bifurcation set of X shows resonances within resonances within resonances. Note that δ_0 depends on the number of times this analysis is repeated, and it will in general tend to zero as this number increases without bounds.

Acknowledgments

The authors wish to thank Claude Baesens, Freddy Dumortier, Heinz Hanßmann, Hans de Jong, Angel Jorba, Hil Meijer, Robert Reid, Floris Takens, Jordi Villanueva and

Table A1. List of bifurcations that occur in the article. The subscript indicates the codimension of the bifurcation. The column 'Incidence' lists the subordinate bifurcations of highest codimension. See [1, 24, 25, 29, 40] for details concerning the terminology and fine structure.

Notation	Name	Incidence
SN_1	Saddle-node	
H_1	Hopf	
PF_1	Pitchfork	
L_1	Homoclinic	
He_1	Heteroclinic	
$SNLC_1$	Saddle-node of limit cycles	
SN_2	Cusp	$SN_1 + SN_1$
H_2	Degenerate Hopf	$SN_1 + SNLC_1$
BT_2	Bogdanov-Takens	$SN_1 + H_1 + L_1$
PF_2	Degenerate Pitchfork	$PF_1 + SN_1$
SDZ_2	Symmetric Double Zero	$PF_1 + H_1$
L_2	Homoclinic at saddle-node	$L_1 + SN_1$
DL_2	Degenerate homoclinic	$L_1 + SNLC_1$
NE_3	Singularity of nilpotent-elliptic type	$SN_2 + BT_2 + L_2 + H_2$

especially Henk Broer and Vincent Naudot for useful discussions and remarks during the preparation of this article.

Appendix A. Bifurcations

Appendix A.1. Nomenclature

In the paper, bifurcation points are indicated by abbreviations of the form $\mathrm{XX}^{letter}_{codim}$, where XX indicates the type of bifurcation, *codim* is a positive integer indicating the codimension, and *letter* is an optional lower case letter indexing a particular bifurcation set. The abbreviations we use are summarised in table A1.

Appendix A.2. Singularities of nilpotent-elliptic type

In this section, which is based entirely on the results of [25], we describe briefly the singularity of elliptic-nilpotent type (NE_3) that occurs in our analysis. For an explanation of the more complicated global bifurcation, we refer the reader to [25].

Consider a 3-parameter family of vector fields of the form

$$\begin{aligned} \dot{x} &= y + \mathsf{O}(|x,y|^4), \\ \dot{y} &= \nu_1 + \nu_2 x + \nu_3 y + \beta_1 x^2 + \beta_2 xy - x^3 + \beta_3 x^2 y + \mathsf{O}(|x,y|^4), \end{aligned} \tag{A.1}$$

where ν_1, ν_2 and ν_3 are parameters, and where β_1, β_2 and β_3 are functions depending only on these parameters. The central singularity $(x, y, \nu_1, \nu_2, \nu_3) = (0, 0, 0, 0, 0)$ of (A.1) is called a NE_3 bifurcation point of elliptic type if $\beta_1(0,0,0) = 0$ and $\beta_2(0,0,0) > 2\sqrt{2}$.

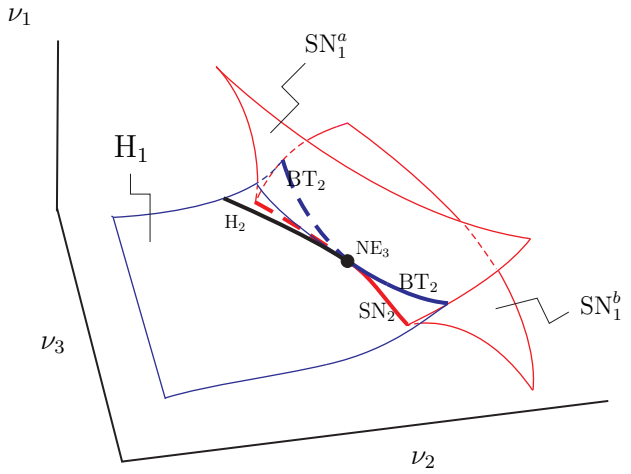


Figure A1. Local bifurcation manifolds of the family (A.1) around a singularity of elliptic-nilpotent type (NE_3).

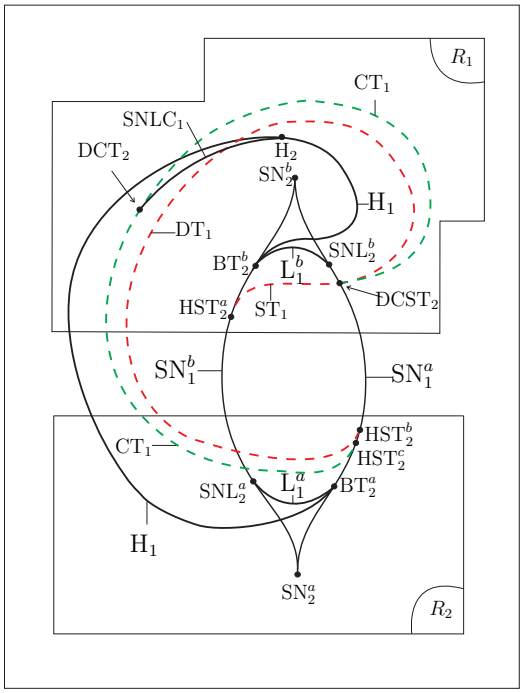


Figure A2. Intersection of local and global bifurcation manifolds of the family (A.1) with a small sphere around a NE_3 point, projected onto the plane. Bifurcations that are not listed in table A1 are explained in the text.

The local bifurcation manifolds of this family at a singularity of elliptic-nilpotent type are given in figure A1. The NE_3 point is an isolated point on the smooth curve of Bogdanov-Takens (BT_2) points; all other points on the curve are non-degenerate. At the NE_3 point the following bifurcation surfaces and curves meet tangently: surfaces of Hopf (H_1) and saddle-node (SN_1^a and SN_1^b) bifurcation points, curves of Bogdanov-Takens (BT_2), cusp (SN_2) and degenerate Hopf (H_2) points. Moreover, the Hopf surface meets the saddle-node surfaces tangently at the Bogdanov-Takens curves. Global bifurcation

manifolds are not indicated.

The bifurcation set of (A.1) is a topological cone with vertex at $0 \in \mathbb{R}^3$. That is, the codimension one surfaces and codimension two curves of the bifurcation set are transversal to the spheres $\nu_1^2 + \nu_2^2 + \nu_3^2 = \varepsilon^2$, for $\varepsilon > 0$ small enough. If S is such a sphere for some fixed value of ε, let Σ the intersection of the bifurcation set with S. The codimension-one bifurcation surfaces intersect S in a finite number of curves on S; the codimension-two curves intersect S in a finite number of points. These points will be either end point or intersection points of bifurcation curves on S.

To obtain figure A2, we delete a point $\{*\}$ from the sphere S and map the punctured sphere $S\backslash\{*\}$ to the plane. The point $\{*\}$ is chosen in the complement of the bifurcation set on the hemisphere $\nu_2 < 0$. We obtain two saddle-node curves SN_1^a and SN_1^b that meet tangently at two cusp points SN_2^a and SN_2^b. The Hopf curve H_1 meets SN_1^a and a (global) curve L_1^a of homoclinic bifurcations tangently at BT_2^a; likewise, it meets SN_1^b and L_1^b tangently at BT_2^b.

A curve of saddle-node bifurcations of limit cycles (SNLC_1) emanates from a degenerate Hopf point on the Hopf curve; the curve SNLC_1 terminates at a double cycle tangency (DCT_2) point. From a double centre separatrix tangency (DCST_2) point emanates a cycle tangency (CT_1) and a double tangency (DT_1) curves. These curves terminate at hyperbolic separatrix tangency points HST_2^b and HST_2^c, respectively. The DCST_2 point and HST_2^a are connected by a separatrix tangency (ST_1) curve. Dashed curves indicate bifurcations which are shown (in [25]) to occur in the family (8), but which are not recovered in the present article.

Appendix B. Averaging over the torus

In this appendix normal forms of the vector fields are computed by averaging at a normal resonance parameter σ_0. Without loss of generality, we may assume that $\sigma_0 = 0$. After applying a van der Pol transformation [9, 16, 36, 39, 51], the vector field can be split in an integrable part and a part that is of high order in the variables $|z|$, $|\sigma|$ and $|\varepsilon|$. Throughout the following, parametrised vector fields $X(\sigma, \varepsilon)$ on M with $\sigma \in P$ and $\varepsilon \in I$ are considered as vertical vector fields X on $\mathcal{M} = M \times P \times I$.

Appendix B.1. Averaging

We consider X as given by equation (5):

$$X = \omega\frac{\partial}{\partial x} + \mathrm{Re}\,\left(\mathrm{i}\alpha_0 + g(|z|^2, \sigma)z + \varepsilon f(x, z, \bar{z}, \sigma, \varepsilon)\right)\frac{\partial}{\partial z},$$

where $g(|z|^2, \sigma) = (\lambda - \mathrm{i}\alpha_0) + g_1|z|^2 + \mathsf{O}(|z|^4)$. From the averaging result below it follows that if $k_0\omega + \ell\alpha_0 = 0$, then there is an 'averaging' coordinate transformation putting X into the form

$$X = \omega\frac{\partial}{\partial x} + \mathrm{Re}\,\left(\mathrm{i}\alpha_0 z + g(|z|^2, \sigma)z + \varepsilon A\,\mathrm{e}^{\mathrm{i}\langle k_0, x\rangle}\bar{z}^{\ell-1} + \varepsilon R\right)\frac{\partial}{\partial z}$$

where $R = \mathsf{O}(\varepsilon, |z|, |\lambda - \mathrm{i}\alpha_0|)$.

To express the result more formally, recall that σ and ε take values in some bounded open neighbourhoods P and I of 0 in $\mathbb{R}^q$ and $\mathbb{R}$ respectively. It is assumed that there is an integer vector $k_0 \in \mathbb{Z}^m \backslash \{0\}$ such that the greatest common divisor of the components of k_0 and ℓ is 1; in particular, if $\ell = 1$, the components of k_0 are mutually prime. Moreover we assume that we have

$$\langle k_0, \omega \rangle + \ell\alpha_0 = 0, \tag{B.1}$$

whereas for all $k \neq k_0$ we have $|\langle k, \omega \rangle + \ell\alpha_0| \geq \gamma(|k|+1)^{-\tau}$. Finally, we introduce

$$\mathsf{O}_n = \mathsf{O}\left(\sum_{2j+|\rho|+r=n} |z|^{2j} |\sigma|^{|\rho|} |\varepsilon|^r \right).$$

Proposition 5. *If $k_0\omega + \ell\alpha_0 = 0$, for ω Diophantine and $\gcd(k_0, \ell) = 1$, then there exists a smooth transformation $\Psi_N = \Psi_N(x, z, \bar{z}, \sigma, \varepsilon)$, mapping X to $Y_N = \Psi_{N*}X$, such that*

$$\begin{aligned} Y_N = \omega\frac{\partial}{\partial x} + \Bigg(& \mathrm{i}\alpha_0 z + G(|z|^2, \sigma, \varepsilon) z \\ & + \varepsilon \sum_{j=0}^{[N/2]} \sum_{r=1}^{[(N+1-2j)/\ell]} A_{jr}(\sigma, \varepsilon)\, \mathrm{e}^{-\mathrm{i}r\langle k_0, x\rangle} |z|^{2j} \bar{z}^{r\ell-1} \\ & + \varepsilon \sum_{j=0}^{[N/2]} \sum_{r=1}^{[(N-2j-1)/\ell]} B_{jr}(\sigma, \varepsilon)\, \mathrm{e}^{\mathrm{i}r\langle k_0, x\rangle} |z|^{2j} z^{r\ell+1} + \mathsf{O}(\varepsilon)\mathsf{O}_N \Bigg) \frac{\partial}{\partial z}, \end{aligned} \tag{B.2}$$

with $G(|z|^2, \sigma, 0) = (\lambda - \mathrm{i}\alpha_0) + g_1|z|^2 + \mathsf{O}(|z|^4)$ and A_{jr} and B_{jr} multinomials in σ and ε of order at most N.

Appendix B.2. Proof of the averaging result

The techniques used in the proof are standard.

Notation. Define the norm $|\gamma|$ of a multi–index $\gamma = (\gamma_1, \cdots, \gamma_n) \in \mathbb{N}^n$ by

$$|\gamma| = \gamma_1 + \cdots + \gamma_n.$$

For the multi-index $\beta = (\beta_1, \beta_2, \beta_3, \beta_4) = (\beta_1, \beta_2, \beta_{31}, \cdots, \beta_{3q}, \beta_4) \in \mathbb{N}^{q+3}$, we write

$$p_\beta(z, \bar{z}, \sigma, \varepsilon) = z^{\beta_1} \bar{z}^{\beta_2} \sigma^{\beta_3} \varepsilon^{\beta_4}.$$

Also, for a multi–index $\tilde{\beta} = (\beta_0, \beta) \in \mathbb{N} \times \mathbb{N}^{q+3}$ and $f = f(x, z, \bar{z}, \sigma, \varepsilon)$, we write

$$\partial_{\tilde{\beta}} f = \frac{\partial^{|\tilde{\beta}|} f}{\partial x^{\beta_0} \partial z^{\beta_1} \partial \bar{z}^{\beta_2} \partial \sigma^{\beta_3} \partial \varepsilon^{\beta_4}}.$$

Induction hypotheses. The transformation Ψ will be constructed as a composition $\Psi = \Phi_N \circ \cdots \circ \Phi_0$ of transformations Φ_n. We proceed by induction. Assume that there exists a smooth transformation $\Psi_n = \Phi_n \circ \cdots \circ \Phi_0$, C^∞–close to the identity, mapping X to

$$Y_n = \Psi_{n*} X.$$

Here

$$Y_n = \omega \frac{\partial}{\partial x} + \mathrm{Re}\Big(\mathrm{i}\alpha_0 z + g(|z|^2, \sigma) \\ + \varepsilon \sum_{I_{n,\ell}} c_\beta \, \mathrm{e}^{\mathrm{i} r_\beta \langle k_0, x\rangle} p_\beta + \varepsilon R_{n+1}(x, z, \bar{z}, \sigma, \varepsilon) \Big) \frac{\partial}{\partial z},$$

with $r_\beta = (\beta_1 - \beta_2 - 1)/\ell$ and with $R_{n+1} = \mathsf{O}_n$ a smooth function. The index set is given by

$$I_{n,\ell} = \left\{ \beta \in \mathbb{Z}^2 \,:\, \beta_1 + \beta_2 \le n, \quad \beta_1 - \beta_2 - 1 \equiv 0 \bmod \ell \right\}.$$

Note that the induction hypothesis is true for $n = 1$ if we set $\Psi_0 = \Phi_0 = \mathrm{id}$, $Y_0 = X$ and $R_1 = f$. If the induction hypothesis is shown to be true for $n = N$, we see that the proposition is proved.

Determining the transformation. We turn to the induction step. Taylor's theorem is used to write:

$$R_n = f_n + \tilde{R}_{n+1} = \sum_{|\beta|=n-1} f_\beta(x) p_\beta + \tilde{R}_{n+1},$$

with $\tilde{R}_{n+1} = \mathsf{O}_n$. We look for a coordinate transform Φ_n of the form:

$$\Phi_n^{-1} = \Big(x, z + \varepsilon u(x, z, \bar{z}, \sigma, \varepsilon), \sigma, \varepsilon \Big) = \left(x, z + \varepsilon \sum_{|\beta|=n-1} u_\beta(x) p_\beta, \sigma, \varepsilon \right).$$

Note that lower order terms are not changed by this transformation, while the general component $\xi \frac{\partial}{\partial z}$ of order n in $\Phi_{n*} Y_{n-1}$ reads as

$$\xi = -\left(\left\langle \frac{\partial u}{\partial x}, \omega \right\rangle + \mathrm{i}\alpha_0 z \frac{\partial u}{\partial z} - \mathrm{i}\alpha_0 \bar{z} \frac{\partial u}{\partial \bar{z}} \right) + \mathrm{i}\alpha_0 u + f_n. \tag{B.3}$$

Writing $\xi = \sum_\beta \xi_\beta p_\beta$, we determine u_β such that as many coefficients ξ_β vanish as possible.

Homological equations. Writing equation (B.3) in components implies the following set of *homological equations* for the u_β:

$$\left\langle \frac{\partial u_\beta}{\partial x}, \omega \right\rangle + \mathrm{i}(\beta_1 - \beta_2 - 1)\alpha_0 u_\beta = f_\beta - \xi_\beta.$$

Fixing β and dropping the subscripts β for a moment, we expand u, f and ξ into Fourier series $\sum u_k \, \mathrm{e}^{\mathrm{i}\langle k, x\rangle}$ etc. and we obtain the following equations for the coefficients u_k:

$$\mathrm{i}\Big(\langle k, \omega \rangle + (\beta_1 - \beta_2 - 1)\alpha_0 \Big) u_k = f_k - \xi_k. \tag{B.4}$$

If $\ell k = (\beta_1 - \beta_2 - 1)k_0$, the fraction $r = (\beta_1 - \beta_2 - 1)/\ell$ is an integer such that $k = rk_0$ and $(\beta_1 - \beta_2 - 1)\alpha_0 = r\ell\alpha_0$. The left hand side of equation (B.4) then vanishes; the equation can in this case be satisfied only if $\xi_k = f_k$. We set

$$\begin{cases} \xi_k = 0 \quad \text{and} \quad u_k = \dfrac{f_k}{\langle k, \omega\rangle + (\beta_1 - \beta_2 - 1)\alpha_0}, \\ \qquad\qquad\quad \text{if} \quad \ell k \neq (\beta_1 - \beta_2 - 1)k_0; \\ \xi_k = f_k \quad \text{and} \quad u_k = 0, \\ \qquad\qquad\quad \text{if} \quad \ell k = (\beta_1 - \beta_2 - 1)k_0. \end{cases} \tag{B.5}$$

To provide a solution for equation (B.4), we show that the series $\sum_k u_k \, \mathrm{e}^{\mathrm{i}\langle k,x\rangle}$ converges. If $k \neq rk_0$ for any r, we find using equation (B.1)

$$\begin{aligned} |\langle k, \omega\rangle + r\ell\alpha_0| &= |\langle k, \omega\rangle + r\ell\alpha_0 - r\left(\langle k_0, \omega\rangle + \ell\alpha_0\right)| \\ &= |\langle k - rk_0, \omega\rangle| \geq \gamma \, |k - rk_0|^{-\tau} . \end{aligned} \tag{B.6}$$

The right hand side of (B.6) is finite if $k \neq rk_0$. Note also that $|r/\ell| = |(\beta_1 - \beta_2 - 1)/\ell|$ is bounded from above by $2n + 1$, and that the following estimate holds true:

$$|k - rk_0| \leq |k| + |r||k_0| \leq C^{\frac{1}{\tau}} \left(|k| + 1\right),$$

where $C^{\frac{1}{\tau}} = (2n + 1)|k_0|$. It follows that

$$|\langle k, \omega\rangle + (\beta_1 - \beta_2 - 1)\alpha_0| \geq \frac{\gamma}{C} \left(|k| + 1\right)^{-\tau}$$

if $\ell k \neq (\beta_1 - \beta_2 - 1)k_0$.

We now re-incorporate the index β. Since f is a smooth function, for every $s > 0$ there is a constant C_s, depending on β and f, such that

$$|f_{k\beta}| \leq C_s \left(|k| + 1\right)^{-s} \quad \text{for all} \quad k \in \mathbb{Z}^m.$$

Using equation (B.5), we have for every $s \geq 0$

$$|u_{k\beta}| \leq \frac{CC_s}{\gamma} \left(|k| + 1\right)^{-s+\tau} \quad \text{for all} \quad k \in \mathbb{Z}^m.$$

Consequently, on a compact neighbourhood K_n of $\mathbb{T}^m \times \{0\} \times \{0\} \times \{0\}$ in $M \times P \times I$, the function u and its derivatives $\partial_{\tilde{\beta}} u$ can be estimated by

$$\begin{aligned} \max_{K_n} |\partial_{\tilde{\beta}} u| &= \max_{K_n} \left| \partial_{\tilde{\beta}} \sum_{|\beta| \leq n} \sum_k u_{k\beta} \, \mathrm{e}^{\mathrm{i}\langle k,x\rangle} p_\beta \right| \\ &\leq \frac{CC_s}{\gamma} \sum_{|\beta| \leq n} \sum_k |k|^{|\tilde{\beta}|} (|k| + 1)^{-s+\tau} \max_{K_n} |p_\beta|. \end{aligned}$$

For s large enough, the right hand side converges. Since $\tilde{\beta}$ was arbitrary, it follows that u, and hence Φ_n is a smooth function. Choosing K_n smaller if necessary, it can be achieved that Φ_n^{-1} is invertible on K_n. ∎

Appendix B.3. Van der Pol transformation

In this section, it is shown how the normal form (B.2) obtained above decouples from the dynamics on the torus if a well–chosen van der Pol transformation is applied to the system; this procedure is also known as 'introducing co-rotating coordinates'. Our treatment is very close to [9], but see also [16].

Co-rotating coordinates. In the case $\ell = 1$, it is sufficient to apply the transformation Ψ to the normal form (B.2) that is given by

$$\Psi^{-1}(x, z, \bar{z}, \sigma, \varepsilon) = \left(x,\, \mathrm{e}^{\mathrm{i}\langle k_0, x\rangle} z,\, \mathrm{e}^{-\mathrm{i}\langle k_0, x\rangle}\bar{z}, \sigma, \varepsilon\right).$$

The transformed vector field $V_N = \Psi_* Y_N$ reads as

$$V_N = \omega\frac{\partial}{\partial x} + \Big(G(|z|^2, \sigma, \varepsilon)z + \varepsilon\sum_{j,r} A_{jr}|z|^{2j}\bar{z}^{r-1} + \varepsilon\sum_{j,r} B_{jr}|z|^{2j}z^{r+1} + \varepsilon R_{N+1}(x, z, \bar{z}, \sigma, \varepsilon)\Big)\frac{\partial}{\partial z},$$

where and $R_{N+1} = \mathsf{O}_N$, A_{jr} and B_{jr} are polynomials in σ and ε of order at most N and $G(|z|^2, \sigma, 0) = (\lambda - \mathrm{i}\alpha_0) + g_1|z|^2 + \mathsf{O}(|z|^4)$.

Covering space. The case $\ell = 2$ (actually, the method is general and works for $\ell \geq 2$) is more involved, since we have to lift the vector field to a covering space of the torus.

First however we simplify the normal form (B.2) further by transforming the torus $\mathbb{T}^m$. We let $\kappa_0 = \gcd(k_0)$ and write $k_0 = \kappa_0\tilde{k}_0$; remark that $\gcd(\kappa_0, \ell) = 1$ by hypothesis. Then $\gcd(\tilde{k}_0) = 1$, and we can find vectors $v_2, \cdots, v_m \in \mathbb{Z}^m$ such that the matrix $U_{\tilde{k}_0} = (\tilde{k}_0\, v_2\, \cdots\, v_m)^t$ is unimodular. Note that if $\tilde{x} = U_{\tilde{k}_0}x$, then in particular

$$\tilde{x}_1 = \left\langle \tilde{k}_0, x\right\rangle = \frac{1}{\kappa_0}\langle k_0, x\rangle.$$

Applying the transformation $(x, z) \mapsto (U_{\tilde{k}_0}x, z)$ to the normal form (B.2) yields then

$$\begin{aligned} Y_N = \left(U_{\tilde{k}_0}\omega\right)\frac{\partial}{\partial x} + \Bigg(&\mathrm{i}\alpha_0 z + G(|z|^2, \sigma, \varepsilon)z \\ &+\varepsilon\sum_{j=0}^{[N/2]}\sum_{r=1}^{[(N+1-2j)/\ell]} A_{jr}(\sigma, \varepsilon)\,\mathrm{e}^{-\mathrm{i}r\kappa_0 x_1}|z|^{2j}\bar{z}^{r\ell-1} \\ &+\varepsilon\sum_{j=0}^{[N/2]}\sum_{r=1}^{[(N-2j-1)/\ell]} B_{jr}(\sigma, \varepsilon)\,\mathrm{e}^{\mathrm{i}r\kappa_0 x_1}|z|^{2j}z^{r\ell+1} + \mathsf{O}(\varepsilon)\mathsf{O}_N\Bigg)\frac{\partial}{\partial z}, \end{aligned} \tag{B.7}$$

Note that the normal form terms that are not of order $\mathsf{O}(\varepsilon)\mathsf{O}_N$ depend now only on one of the torus angles; that is, the principal perturbation in this normal form is now seen to be periodic instead of quasi-periodic.

By lifting the normal form (B.7) to a ℓ-fold covering space, even the x_1-dependence can be made to disappear. The covering transformation $\Psi : \mathbb{T}^m \times \mathbb{C} \to \mathbb{T}^m \times \mathbb{C}$ reads as

$$\Psi(x, z) = (\ell x_1, x_2, \cdots, x_m, \mathrm{e}^{\mathrm{i}\kappa_0 x_1} z).$$

As always, the x_j-coordinates are taken modulo 2π. Note that this map is ℓ-to-one. The vector field $\tilde{Y}_N$ is a lift of Y_N under this map if

$$\Psi_* \tilde{Y}_N = Y_N.$$

The expression $\Psi_* \tilde{Y}_N$ yields a well-defined vector field only if $\tilde{Y}_N$ is symmetric with respect to the group $\mathbb{Z}_\ell$ of deck transformations that is generated by

$$(x, z) \mapsto \left(x_1 + \frac{2\pi}{\ell}, \mathrm{e}^{-\mathrm{i}\kappa_0 2\pi/\ell} z \right).$$

With this specification, there is a unique vector field $\tilde{Y}_N$ such that $\Psi_* \tilde{Y}_N = Y_N$. We have

$$\begin{aligned} \tilde{Y}_N = \frac{1}{\ell} \left(U_{\tilde{k}_0} \omega \right) \frac{\partial}{\partial x} + \Bigg(& \mathrm{i}\alpha_0 z + G(|z|^2, \sigma, \varepsilon) z \\ & + \varepsilon \sum_{j=0}^{[N/2]} \sum_{r=1}^{[(N+1-2j)/\ell]} A_{jr}(\sigma, \varepsilon) |z|^{2j} \bar{z}^{r\ell - 1} \\ & + \varepsilon \sum_{j=0}^{[N/2]} \sum_{r=1}^{[(N-2j-1)/\ell]} B_{jr}(\sigma, \varepsilon) |z|^{2j} z^{r\ell+1} + \mathsf{O}(\varepsilon) \mathsf{O}_N \Bigg) \frac{\partial}{\partial z}, \end{aligned} \tag{B.8}$$

Note that since $\gcd(\kappa_0, \ell) = 1$, the terms of order lower than $\mathsf{O}(\varepsilon)\mathsf{O}_N$ are symmetric with respect to the group $\mathbb{Z}_\ell$ generated by

$$(x, z) \mapsto \left(x, \mathrm{e}^{2\pi \mathrm{i}/\ell} z \right).$$

Appendix C. Nondegeneracy checking

In this section all coefficients are given that appear in the normal form calculations of the proof of propostion 2. The coefficients appearing in equation (18) are functions of α, μ, ϑ and the equilibrium (y_{10}, y_{20}). They are given by

$$\begin{aligned} a_1 &= \quad \mu + (y_{10}^2 + y_{20}^2) \cos\vartheta + 2y_{10}(y_{10}\cos\vartheta - y_{20}\sin\vartheta), \\ a_2 &= -\alpha - (y_{10}^2 + y_{20}^2) \sin\vartheta + 2y_{20}(y_{10}\cos\vartheta - y_{20}\sin\vartheta), \\ b_1 &= \quad \alpha + (y_{10}^2 + y_{20}^2) \sin\vartheta + 2y_{10}(y_{10}\sin\vartheta + y_{20}\cos\vartheta), \\ b_2 &= \quad \mu + (y_{10}^2 + y_{20}^2) \cos\vartheta + 2y_{20}(y_{10}\sin\vartheta + y_{20}\cos\vartheta), \end{aligned}$$

$$\begin{aligned} a_3 &= 3y_{10}\cos\vartheta - \ y_{20}\sin\vartheta, & b_3 &= \ y_{20}\cos\vartheta + 3y_{10}\sin\vartheta, \\ a_4 &= 2y_{20}\cos\vartheta - 2y_{10}\sin\vartheta, & b_4 &= 2y_{10}\cos\vartheta + 2y_{20}\sin\vartheta, \\ a_5 &= \ y_{10}\cos\vartheta - 3y_{20}\sin\vartheta, & b_5 &= 3y_{20}\cos\vartheta + \ y_{10}\sin\vartheta, \\ a_6 &= \cos\vartheta, & a_7 &= -\sin\vartheta. \end{aligned}$$

In the proof of proof of proposition 2, we referred to the appendix the computation of the coefficient $\operatorname{Re} C_2$. The coefficients B_i in equation (19) are functions of the a_j and b_j. They are given by

$$
\begin{aligned}
B_1 = \frac{1+i}{8a_2^2}\Big(& a_5(a_1-b_2)^2 + a_2(2a_2a_3 - a_1a_4 + 2a_5b_1 + a_4b_2) \\
&+\Big(a_5(a_1-b_2) - a_2a_4\Big)\sqrt{4a_2b_1 + (a_1-b_2)^2}\Big) \\
B_2 = \frac{1+i}{4a_2}\,& (2a_2a_3 - a_1a_4 - 2a_5b_1 + a_4b_2) \\
B_3 = \frac{1+i}{8a_2^2}\Big(& a_5(a_1-b_2)^2 + a_2(2a_2a_3 - a_4a_1 + 2a_5b_1 + a_4b_2) \\
&-\Big(a_5(a_1-b_2) - a_2a_4\Big)\sqrt{4a_2b_1 + (a_1-b_2)^2}\Big) \\
B_4 = \frac{1+i}{128a_2^3}\Big(& 8a_2a_6((a_1-b_2)^2 + 2a_2^2 + a_2b_1) \\
&-a_7(a_1-b_2)(5(a_1-b_2)^2 + 8a_2^2 + 12a_2b_1) \\
&+ i((a_1-b_2)^2 + 4a_2b_1)(2a_2a_6 - 3a_7(a_1-b_2)) \\
&+8\Big(a_2a_6(a_1-b_2) - a_7(a_1-b_2)^2 \\
&\quad -a_2a_7(a_2+b_1)\Big)\sqrt{4a_2b_1 + (a_1-b_2)^2}\Big) \\
B_5 = \frac{1+i}{128a_2^3}\Big(& 3a_7(a_1-b_2)(4a_2b_1 - (a_1-b_2)^2 - 8a_2^2) \\
&+2a_2a_6(5(a_1-b_2)^2 + 24a_2^2 - 4a_2b_1) \\
&- i((a_1-b_2)^2 + 4a_2b_1)(2a_2a_6 - 3a_7(a_1-b_2)) \\
&+8(a_2a_6(a_1-b_2) + a_2a_7(2b_1 - a_2))\sqrt{4a_2b_1 + (a_1-b_2)^2}\Big) \\
B_6 = \frac{1+i}{128a_2^3}\Big(& 3a_7(a_1^3 - b_2^3) + a_2^3(58a_6 + 24a_7) \\
&-a_2^2(a_1a_7 + 8a_6b_1 - 9a_7b_2) - a_1b_2(20a_2a_6 + 9a_7b_2) \\
&- 2a_2(6a_1a_7b_1 + b_2(3a_7b_1 - 5a_6b_2)) \\
&+ i(3a_7(a_1^3 - b_2^3) - a_1b_2(4a_2a_6 + 9a_7b_2) \\
&+ a_2^2(8a_6b_1 - a_1a_7 + 9a_7b_2 + 2a_2a6) \\
&- 2a_2(6a_1a_7b_1 + b_2(3a_7b_1 - a_6b_2))) \\
&-8(a_2a_6(a_1-b_2) + a_2a_7(2b_1 + a_2))\sqrt{4a_2b_1 + (a_1-b_2)^2}\Big) \\
B_7 = \frac{1+i}{128a_2^3}\Big(& 8a_2a_6\Big((a_1-b_2)^2 + 2a_2^2 + a_2b_1\Big) \\
&- a_7(a_1-b_2)\Big(5(a_1-b_2)^2 + 8a_2^2 + 12a_2b_1\Big)
\end{aligned}
$$

$$
\begin{aligned}
&+ i((a_1-b_2)^2+4a_2b_1)(2a_2a_6-3a_7(a_1-b_2))\\
&+ 8\Big(a_7(a_1-b_2)^2+a_2a_7(a_2+b_1)\\
&-a_2a_6(a_1-b_2)\Big)\sqrt{4a_2b_1+(a_1-b_2)^2}\Big)
\end{aligned}
$$

and

$$
\begin{aligned}
\mathrm{Re}\,(C_2) = &-12\mathrm{Im}\,(B_4B_6)\\
&+\frac{1}{\mathrm{Im}\,\lambda}\Big[\mathrm{Re}\,\Big(12(B_6-\overline{B}_4)+8B_3(\overline{B}_6-B_4)+12\overline{B}_3B_7\\
&\qquad +20B_2\overline{B}_3\overline{B}_4+12B_2\overline{B}_3B_6+4B_2B_3\overline{B}_7\\
&\qquad -24B_2^2B_4)\Big)+12\mathrm{Im}\,B_1B_2\mathrm{Im}\,B_5\Big]\\
&+\frac{2}{(\mathrm{Im}\,\lambda)^2}\Big[\mathrm{Im}\,\Big(4\overline{B}_1^2B_2\overline{B}_3-6\overline{B}_1B_2^2\overline{B}_3-B_2^3\overline{B}_3\Big)\\
&\qquad +6\mathrm{Re}\,(B_1B_2)\mathrm{Im}\,(B_2\overline{B}_3)-8|B_3|^2\mathrm{Im}\,(B_2\overline{B}_3)\Big].
\end{aligned}
$$

By using the MATHEMATICA package [56], we have established that at the degenerate Hopf point the coefficient $\mathrm{Re}\,C_2$ does not vanish. This implies that there are no doubly degenerate Hopf points in the present model.

We end this section by giving the coefficients of the normal form (23) which are also functions of α, μ, ϑ and the equilibrium (x_0, y_0):

$$
\begin{aligned}
K_1 &= a_5b_1^2,\\
K_2 &= a_4b_1+2b_1b_5,\\
K_3 &= a_5b_1^2b_4-a_4b_1^2b_5+a_7b_1^3,\\
K_4 &= -a_5b_1b_3+\frac{5}{2}a_3a_4b_1+\frac{1}{2}a_4b_1b_4-5a_3b_1b_5+4a_6b_1^2-4b_1b_4b_5,\\
K_5 &= -5a_3b_1^2b_5^2-3a_6b_1^3b_5+\frac{5}{4}a_5b_1^2b_4^2+\frac{35}{12}a_3^2a_5b_1^2-2a_1a_2a_7b_1b_5\\
&\quad -\frac{2}{3}a_5b_1^2b_3b_5-\frac{4}{3}a_3a_5b_1^3b_5+\frac{1}{3}a_4a_5b_1^2b_3+\frac{1}{3}a_4a_5b_1^3b_4+\frac{3}{2}a_7b_1^3b_4\\
&\quad +\frac{5}{2}a_3a_7b_1^3-\frac{2}{3}a_5b_1^4b_5^2-\frac{1}{3}a_5a_7b_1^3-a_4a_6b_1^3+\frac{23}{6}a_3a_5b_1^2b_4\\
&\quad -\frac{1}{2}a_4b_1^2b_4b_5-\frac{5}{2}a_3a_4b_1^2b_5,\\
K_6 &= -\frac{1}{6}\Big(4a_3a_4b_1b_5-8a_4b_1b_4b_5-56b_3b_5^2+32a_3^2b_5+2a_4^2b_3-66a_6b_1b_4\\
&\quad -84a_3a_6b_1-24a_7b_1b_3-18a_7b_1^3b_5+30b_4^2b_5-26a_3^2a_4-3a_4b_4^2\\
&\quad +4b_1^2b_5^3+42a_4b_3b_5-13a_3a_4b_4+52a_3b_4b_5-108a_3a_5b_3\\
&\quad -60a_5b_3b_4-28a_7b_1b_5-12a_5a_6b_1-4a_4^2b_1b_4+8a_3b_1b_5^2\\
&\quad -2a_4a_7b_1+2a_4b_1^2b_5^2\Big).
\end{aligned}
$$

A simple computation shows that K_2 never vanishes on the Bogdanov-Takens bifurcation curves. We conclude that degenerate cusp bifurcation do not occur in the family $\mathrm{Re}\,(\lambda z+ \mathrm{e}^{\mathrm{i}\vartheta}|z|^2z+1)\frac{\partial}{\partial z}$.

[1] V.I. Arnol'd, *Geometrical methods in the theory of ordinary differential equations. Second Edition*, Springer 1988.

[2] C. Baesens, J. Guckenheimer, S. Kim and R. MacKay, Simple resonance regions of torus diffeomorphisms, In: Patterns and Dynamics of Reactive Media (Aris, Aronson and Swinney eds.), *IMA Volumes in Mathematics and its Applications* **37** (1991), 1-11.

[3] B.L.J. Braaksma and H.W. Broer, On a quasi-periodic Hopf bifurcation, *Annales de l'Institut Henri Poincaré-Analyse non linéaire* **4** (1987), 115-168.

[4] R.I. Bogdanov, Bifurcations of a limit cycle of a family of vector fields in the plane, *Trudy Seminara Imeni I.G. Petrovskogo* **2** (1976), 23–36, Translation: Selecta Math. Sovietica **1** (1981), 373–388.

[5] R.I. Bogdanov, A versal deformation of a singular point of a vector field in the plane in the case of vanishing eigenvalues, *Trudy Seminara Imeni I.G. Petrovskogo* **2** (1976), 37–65, Translation: Selecta Math. Sovietica **1** (1981), 389–421.

[6] H.W. Broer, Notes on perturbation theory 1991, Erasmus ICP *Mathematics and Fundamental Applications*, Aristotle University Thessaloniki (1993), 44 p.

[7] H.W. Broer, Quasi-periodic bifurcations, applications, *Proc. XI C.E.D.Y.A. (Málaga)* Universidad de Málaga (1989), 3-22.

[8] H.W. Broer, M. Golubitsky and G. Vegter, The geometry of resonance tongues: a singularity theory approach, *Nonlinearity* **16** (2003), 1511-1538.

[9] H.W. Broer, H. Hanßmann, A. Jorba, J. Villanueva and F.O.O. Wagener, Normal-internal resonances in quasi-periodically forced oscillators: a conservative approach, *Nonlinearity* **16** (2003), 1751-1791.

[10] H.W. Broer, G.B. Huitema and M.B. Sevryuk, Quasi-periodic motions in families of dynamical systems, *LNM* **1645**, Springer-Verlag 1996.

[11] H.W. Broer, G.B. Huitema, F.Takens and B.L.J. Braaksma, Unfolding and bifurcations of quasi-periodic tori, *Memoirs of the AMS* **421** (1990).

[12] H.W. Broer, V. Naudot, R. Roussarie and K. Saleh, A predator-prey model with non-monotonic response function, *Regular & Chaotic Dynamics* **11** (2006), 155-165.

[13] H.W. Broer, V. Naudot, R. Roussarie, K. Saleh and F.O.O. Wagener, Organising centres in the semi-global analysis of dynamical systems, *Preprint* 2006.

[14] H.W. Broer, V. Naudot, R. Roussarie and F.O.O. Wagener, Quasi-periodic bifurcations of planar maps, *In preparation* 2005.

[15] H.W. Broer and F.Takens, Formally symmetric normal forms and genericity, *Dynamics Reported* **2** (1989), 39-59.

[16] H.W. Broer and G. Vegter, Bifurcational aspects of parametric resonance, *Dynamics Reported (New Series)* **1** (1992), 1-53.

[17] M.L. Cartwright, Forced oscillations in nearly sinusoidal systems, *Journal of the Institute of Electrical Engineers* **95** (1948), 88–94.

[18] M.L. Cartwright and J.E. Littlewood, On nonlinear differential equations of the second order, I: The equation $\ddot{y} + k(1-y^2)\dot{y} + y = b\lambda k\cos(\lambda t + a)$, k large, *Journal of the London Mathematical Society* **20** (1945), 180–189.

[19] A. Chenciner, Bifurcations de points fixes elliptiques. I. Courbes invariantes, *IHES–Publications mathématiques* **61** (1985), 67-127.

[20] A. Chenciner, Bifurcations de points fixes elliptiques. II. Orbites periodiques et ensembles de Cantor invariants, *Inventiones mathematicae* **80** (1985), 81-106.

[21] A. Chenciner, Bifurcations de points fixes elliptiques. III. Orbites periodiques de 'petites' périodes et élimination résonnante des couples de courbes invariantes, *IHES–Publications mathématiques* **66** (1988), 5-91.

[22] E.J. Doedel, R.A. Champneys, T.F. Fairgrieve, Yu.A. Kuznetsov, B. Sandstede and X.J. Wang, AUTO2000: Continuation and bifurcation software for ordinary differential equations (with HomCont), User's Guide, Concordia University, Montreal, Canada 1997–2000. (*http//indy.cs.concordia.ca*).

[23] F. Dumortier, Local study of planar vector fields, *Studies In Mathematical Physics* **2**, Elsevier Science Publising 1991.

[24] F. Dumortier, R. Roussarie and J. Sotomayor, Generic 3–parameter families of vector fields on the plane, unfolding a singularity with nilpotent linear part. The cusp case, *Ergodic theory and dynamical systems* **7** (1987), 375–413.

[25] F. Dumortier, R. Roussarie, J. Sotomayor and H. Zoladek, Bifurcations of planar vector fields, *LNM* **1480**, Springer-Verlag 1991.

[26] M. Friedman, Quasi-periodic solutions of nonlinear ordinary differential equations with small damping, *Bulletin of the American Mathematical Society* **73** (1967), 460-464.

[27] J.M. Gambaudo, Perturbation of a Hopf bifurcation by an external time-periodic forcing, *Journal of Differential Equations* **57** (1985) 172-199.

[28] W. Govaerts, Y.A. Kuznetsov and A. Dhooge, Numerical continuation of bifurcations of limit cycles in MATLAB. *Preprint* 2003.

[29] J. Guckenheimer and P. Holmes, *Nonlinear oscillations, dynamical systems and bifurcation of vector fields*, Springer-Verlag 1983.

[30] H. Hanßmann, Local and semi-local bifurcations in hamiltonian dynamical systems, results and examples. *Habilitationsschrift*, RWTH Aachen 2004.

[31] D. Hanselman, *Mastering MATLAB*, University of Maine 2001. (http://www.mathworks.com).

[32] M.W. Hirsch and S. Smale, *Differential equations, dynamical systems, and linear algebra*, Academic Press Inc. 1970.

[33] P. Holmes and D. Rand. Bifurcations of the forced van der Pol oscillator. *Quarterly of Applied Mathematics* **35** (1978), 495-509.

[34] À Jorba and C. Simó, On quasi-periodic perturbations of elliptic equilibrium points, *SIAM Journal of Mathematical Analysis* **27** (1996), 1704-1737.

[35] À Jorba and J. Villanueva, On the persistence of lower-dimensional invariant tori under quasi-periodic perturbations, *Journal of Nonlinear Science* **7** (1997), 427-473.

[36] B. Krauskopf, Bifurcation sequences at $1:4$ resonance: an inventory, *Nonlinearity* **7** (1994), 1073-1091.

[37] B. Krauskopf, The bifurcation set for the $1:4$ resonance problem, *Experimental Mathematics* **3**:2 (1994), 107-128.

[38] B. Krauskopf, Bifurcations at ∞ in a model for $1:4$ resonance, *Ergodic Theory and Dynamical Systems* **17**:4 (1997), 899-931.

[39] B. Krauskopf, Strong resonances and Takens's Utrecht preprint, In H.W. Broer, B. Krauskopf, and G. Vegter (Eds.), *Global Analysis of Dynamical Systems, Festschrift dedicated to Floris Takens for his 60th birthday*, Institute of Physics, Bristol and Philadelphia (2001), 89-111.

[40] Y.A. Kuznetsov, *Elements of applied bifurcation theory*, Springer-Verlag 1995.

[41] Y.A. Kuznetsov and H.G.E. Meijer, Remarks on interacting Neimark-Sacker bifurcations, *Preprint* 2006.

[42] J.W. Milnor, *Topology from a differential viewpoint*, The University Press of Virginia 1990.

[43] J. Moser, Combination tones for Duffing's equation, *Communications of Pure and Applied Mathematics* **18** (1965), 167–181.

[44] K. Saleh, *Organising centres in the semi-global analysis of dynamical systems*, Ph.D. thesis, University of Groningen 2005.

[45] J.A. Sanders and F. Verhulst, *Averaging methods in nonlinear dynamical systems*, Springer-Verlag 1985.

[46] J.J. Stoker, *Nonlinear vibrations in mechanical and electrical systems*, Interscience 1950.

[47] F. Takens, Forced oscillations and bifurcations, *Applications of global analysis I* Communications of the Mathematical Institute Rijksuniversiteit Utrecht **3** (1974), 1-59.
In H.W. Broer, B. Krauskopf, and G. Vegter (Eds.), *Global analysis of dynamical systems, Festschrift dedicated to Floris Takens for his 60th birthday*, Institute of Physics, Bristol and Philadelphia (2001), 89-111.

[48] F. Takens, Singularities of vector fields, *IHES–Publications mathématiques* **43** (1974), 47-100.
[49] F. Takens, Unfoldings of certain singularities of vector fields. Generalized Hopf bifurcation, *Journal of Differential Equations* **14** (1973), 476-493.
[50] F. Takens and F.O.O. Wagener, Resonances in skew and reducible quasi-periodic Hopf bifurcations, *Nonlinearity* **13** (2000), 377-396.
[51] B. van der Pol, Forced oscillations in a circuit with nonlinear resistance (receptance with reactive triode), *London, Edinburgh and Dublin Philosophical Magazine* **3** (1927), 65-80.
[52] F.O.O. Wagener, On the quasi-periodic d-fold degenerate bifurcations, *Journal of Differential Equations* **216** (2005), 261-281.
[53] F.O.O. Wagener, Semi-local analysis of the k:1 and k:2 resonances in quasi-periodically forced system. In H.W. Broer, B. Krauskopf, and G. Vegter (Eds.), *Global Analysis of Dynamical Systems, Festschrift dedicated to Floris Takens for his 60th birthday*, Institute of Physics, Bristol and Philadelphia (2001), 113-129.
[54] F.O.O. Wagener, A parametrised version of Moser's modifying terms theorem. *In preparation* 2005.
[55] S. Wiggins, *Introduction to applied nonlinear dynamical systems and chaos*, Springer-Verlag 1980.
[56] S. Wolfram, *The Mathematica book*, Cambridge University Press, Wolfram research Inc. 1996. (http://www.wolfram.com).